

https://dspace.org/

The geochemical and strontium isotope characterisation of South African combustion fly ash and their potential environmental effects

Skhosana, Lungile Charmain

2023

https://hdl.handle.net/10539/35663

Downloaded from a DSpace repository. https://dspace.org/

THE GEOCHEMICAL AND STRONTIUM ISOTOPE CHARACTERISATION OF SOUTH AFRICAN COMBUSTION FLY ASH AND THEIR POTENTIAL ENVIRONMENTAL EFFECTS

By

Lungile Charmain Skhosana

(Student number: 1443419)

Under the supervision of:

Dr. Linda Iaccheri

A research report submitted to the Faculty of Science, University of the Witwatersrand, Johannesburg, in partial fulfilment of the requirements for the degree of Master of Science



UNIVERSITY OF THE
WITWATERSRAND,
JOHANNESBURG

Department of Animal, Plant, and Environmental Sciences
University of the Witwatersrand
Johannesburg

March 2023

Declaration

I declare that this research report is my own, unaided work. It is being submitted for the Degree of Master of Science at the University of the Witwatersrand, Johannesburg. It has not been submitted before for any degree or examination at any other University.

Signature:  Date: 23rd of March 2023

Abstract

The mining of coal in South Africa has played, and continues to play, a vital role in building the country's economy for over a century and a half. During the combustion of low-grade coal for energy production, a large amount of coal utilisation by-products (CUP), such as bottom ash (BA), coal fly ash (CFA), and flue-gas desulfurization gypsum, are generated. Coal-fired power stations in South Africa produce over 25 Mt of CFA per year, with only ca. 5% being re-utilised for building concrete, agriculture, construction, and backfilling mines. The long-term exposure to weathering of CFA poses pressure on environmental systems. Therefore, a better characterisation of the mineralogy and trace element chemical compositions of CFA, and their potential environmental effects have become increasingly important.

Mineralogical and geochemical analyses were carried out on CFA samples sourced from five South African coal-fired power stations: Kriel, Tutuka, Grootvlei, Hendrina, and Komati. The samples were analysed using X-Ray Diffractometry (XRD), X-Ray Fluorescence (XRF) and Inductively Coupled Plasma Mass Spectrometry (ICP-MS). Samples from Tutuka and Kriel Power Stations have been characterised by Strontium (Sr) isotopic analyses. CFA samples of Kriel, Tutuka, Grootvlei, and Hendrina are classified as Class F and alumina-silicate type CFA. The Komati sample is classified as Class N and silico-aluminate type CFA.

The trace elements results indicated variability in the toxic elements among the samples with relatively high concentrations of Cr being detected, along with an abundance of transitional metals. These Cr and transitional metal abundances are higher than the Coal Clarke values for CFA determined by Ketris and Yudovich (2009) and thus pose a potential environmental hazard.

The Sr isotopic characterisation of bulk CFA has contributed towards using Sr as an environmental tracer for CFA in various parts of the world. However, no such investigation of Sr isotopes as an environmental tracer has been undertaken in South Africa before the current investigation. The results obtained, therefore, form the basis for future studies into the leaching behaviour and mobility of Sr and toxic trace elements. The Sr contents for the five coal-fired power stations range between 810.3

ppm and 1759.0 ppm, ranking higher than the global mean value of ca. 740 ppm (Ketris & Yudovich, 2009) for Sr in CFA. Therefore, the studied CFA may have the potential of being environmentally hazardous; consequently, a leaching procedure would need to be conducted to fully understand the correlation between Sr and the mobility of toxic trace elements.

The study into the potential of the Grootvlei, Hendrina, Komati, Tutuka and Kriel CFA as REE sources indicated that the CFA does not qualify as a potential REE source according to the criteria set out by Dai et al. (2017). However, in comparison to REE ore deposits it was discovered that although REY enrichment may be low in the CFA's, the abundance of CFA far exceeds that of REE ore deposits. Therefore, CFA stockpiles can be considered as potential low-grade disseminated REY mineralisations.

Dedication

I would like to dedicate this research report to my late mother and father, Nokhisimusi and Msebenzi Skhosana. The foundation of unconditional love, support, and encouragement that you showed me has carried me to where I stand today.

Acknowledgements

Firstly, I would like to thank the Almighty God, my family, and my friends for the encouragement and support they've shown me despite all the obstacles faced along the way.

I would like to express my sincerest gratitude to my supervisor Dr. Linda Iaccheri for her continued support, guidance, and encouragement, and for assisting me in conducting the Rb-Sr separation at the Wits Isotope Geoscience Laboratory (WIGL) at the School of Geoscience, University of the Witwatersrand.

My sincerest appreciation goes out to Prof. Sehliselo Ndlovu and her research assistant, Ms. Amanda Qinisile Vilakazi, from the School of Chemical and Metallurgical Engineering, University of the Witwatersrand for assisting me in acquiring coal fly ash from the Tutuka and Kriel coal-fired power stations, Prof. Nicola Wagner from the Department of Geology, University of the Johannesburg for assisting in acquiring coal fly ash samples from the Grootvlei and Hendrina coal-fired power stations and lastly, Dr. Sehai Mokhahlane from the School of Chemical and Metallurgical Engineering, University of the Witwatersrand for assisting in acquiring coal fly ash from the Komati coal-fired power station. This study would not have been possible without the assistance and generosity of the aforementioned individuals.

I would like to thank Professor Dave Billing and his Master's candidate students, Mr. Zwivhuya Muntswu and Mr. Tanner Kerspuy, from the School of Chemistry, University of the Witwatersrand, for assisting in conducting and interpreting the XRD analyses on the coal fly ash samples and Mr. Marlin Patchappa from the Earth Lab, School of Geosciences, University of the Witwatersrand, for conducting the ICP-MS and XRF analyses on the coal fly ash samples. From the University of Johannesburg, Department of Geology, I would like to thank Ms. Henriette Ueckermann for assisting in the measurement results for the Rb-Sr extracts.

Table of Contents

List of Figures i
List of Tables iii
List of Acronyms/Abbreviations iv
CHAPTER 1 - Introduction 1
1.1 Background and problem identification 1
1.2 Aims and Objectives 4
CHAPTER 2 – Literature Review 5
2.1 Previous chemical studies on coal fly ashes in South Africa 6
2.2 Chemical and Sr isotopic compositions of coal fly ashes: case studies from overseas 8
2.3 Potential extraction of REE from CFA studies in South Africa 9
2.4 Potential extraction of REE from CFA in other countries 11
CHAPTER 3 – Methodology 13
3.1 Sample selection 13
3.2 Powder X-Ray Diffractometry (PXRD) 14
3.3 X-Ray Fluorescence (XRF) Analysis 15
3.4 Trace elements and REE analysis 16
3.5 Radiogenic Strontium Isotope Analysis 19
CHAPTER 4 - Results 22
4.1 Powder X-Ray Diffractometry (PXRD) 22
4.2 Major element compositions 24
4.3 Trace element compositions 25
4.4 Rare earth elements concentrations 29
4.5 Strontium isotopic compositions 31
CHAPTER 5 - Discussion 33
5.1 Comparison of the mineral assemblages of the studied CFA samples 33
5.2 Potentially hazardous trace elements in CFA 34
5.3 Classification of the CFA samples 36
5.4 Strontium isotopic compositions 39
5.5 CFA as a potential source of REE 43
CHAPTER 6 48
6.1 Conclusion 48
6.2 Limitations 50
6.3 Recommendations 51
References 52

List of Figures

Figure 1: The CFA samples focus of this study were obtained from five different coal-fired power stations in the Mpumalanga Province of South Africa. 13
Figure 2: The Brucker D2 Phaser Powder X-Ray Diffractometer (PXRD) at The School of Chemistry, University of the Witwatersrand 14
Figure 3A and B: The Thermo Scientific iCAP RQ used for the ICP-MS trace elements analysis at the Earth Lab at The University of the Witwatersrand; C) ionising chamber; D) auto sampler for the introduction of the sample solution into the ionising chamber of the iCAP. . 18
Figure 4: PXRD results for CFA from Grootvlei Power Station (M = Mullite, Q = Quartz Low, H = Hematite) 22
Figure 5: PXRD results for CFA from Hendrina Power Station (M = Mullite, Q = Quartz Low, H = Hematite, Ma = Magnetite) 23
Figure 6: PXRD results for CFA from Komati Power Station (E = Ettringite, M = Muliite, Q = Quartz Low, H = Hematite, Ma = Magnetite) 23
Figure 7: PXRD results for CFA from Tutuka and Kriel power stations indicating the presence of quartz, hematite, magnetite, mullite and ettringite. 24
Figure 8: Graph illustrating the trace element concentrations of the CFA normalised to the typical global values for CFA by Ketris and Yudovich (2009) 26
Figure 9: Upper continental crust (UCC) normalised UCC REY + Sc values of the Grootvlei, Hendrina, Komati, Tutuka, Kriel and Coal Clarke Value samples (UCC data from Taylor and McLennan, 1985. Coal Clark Values from Ketris and Yudovich (2009) 29
Figure 10: Concentrations of REY + Sc in the CFA of South African coal-fired power stations, arranged from light to heavy lathanides followed by Y and Sc in ppm 30
Figure 11: Variations in the strontium isotope composition of the CFA from the Tutuka and Kriel samples 31
Figure 12: Potentially toxic trace elements plotted with Sr to show relationship between Sr and toxic trace element concentrations. 32
Figure 13: Potentially toxic trace elements detected in the studied CFA samples that were normalised to the typical global values set out by Ketris and Yudovich (2009) 35
Figure 14: Strontium concentrations of bulk fly ash in this study are compared with data from different coal basins in the United States of America APP: Appalachian Basin, ILL: Illinois Basin and PRB: Powder River Basin (modified from Wang et al., 2020). 40
Figure 15: Comparison of the $^{87}Sr/^{86}Sr$ ratios of bulk ash fly ash samples sourced from different coal basins in the United States of America. APP: Appalachian Basin, ILL: Illinois

Basin, and PRB: Powder River Basin and the data of this study from Tutuka and Kriel (modified from Wang et al., 2020)..... 41
Figure 16: Correlation between Sr and the potentially toxic trace elements within the CFA samples 42
Figure 17: The normalised UCC REY + Sc values of the Grootvlei, Hendrina and Komati sample along with the normalised UCC REY + Sc (incl. Jungar Power Station sourced from Dai et al., 2010) of the CFA samples sourced from the Wagner and Matiane (2018) study (UCC data from Taylor and McLennan, 1985)..... 45
Figure 18: Diagram showing the different clusters for potential REY sources: I. unpromising sources; II. promising sources; and III. highly promising sources with 1 – REE-rich coal ashes; 2 – carbonatite deposits; 3 – hydrothermal deposits and; 4 – weathered crust elution-deposited (ion-absorbed) deposits and the blue star being the CFA in this study (Modified from Seredin and Dai, 2012) 46
Figure 19: Comparison of the normalised UCC REY values of the Grootvlei, Hendrina and Komati CFA samples with values of the REE ore deposits sourced from the Harmer and Nex (2016) (UCC data from Taylor and McLennan, 1985)..... 47

List of Tables

Table 1: Table of the international rock reference material that were prepared in-house from the USGS series (USA) and NIM series (South Africa)…….. 15

Table 2: Comparison of measured and recommended values for USGS reference materials measured among the samples……..... 17

Table 3: Sample weights for the CFA samples and reference material AGV2…… 19

Table 4: The calibration elution scheme for the chemical separation and purification of Rb and Sr from the matrix elements…… 20

Table 5: Major elemental compositions (wt%) of CFA……... 25

Table 6: Trace elemental compositions (ppm) of the CFA samples…… 28

Table 7: Results 87Sr/86Sr ratios for CFA samples……... 31

Table 8: Chemical requirements for different classes of CFA (ASTM International, 2017)…… 37

Table 9: CFA classification criteria as discussed in Vassilev and Vassileva (2007)…… 39

Table 10: Correlation between Sr and the heavy metals detected within the CFA samples…… 42

Table 11: Comparison of the REY + Sc between the upper continental crust (UCC) values from Taylor and McLennan (1985) and the CFA samples from the South African coal-fired power stations…… 44

List of Acronyms/Abbreviations

AMD	Acid Mine Drainage
APP	Appalachian Basin
BA	Bottom Ash
CFA	Coal Fly Ash
CUP	Coal Utilisation By-Product
e.g.	For example
Excl.	Excluding
FA	Fly Ash
HREE	Heavy Rare Earth Elements
ICP-MS	Inductively Coupled Plasma Mass Spectrometry
i.e.	That is
ILL	Illinois Basin
LREE	Light Rare Earth Elements
MKB	Main Karoo Basin
MREE	Medium Rare Earth Elements
Mt	Million tons
PRB	Powder River Basin
REE	Rare Earth Elements
REY	Rare Earth Elements plus Yttrium
UCC	Upper Continental Crust
XRD	X-Ray Diffractometry
XRF	X-Ray Fluorescence
HREE	Heavy Rare Earth Elements

CHAPTER 1 - Introduction

1.1 Background and problem identification

Coal mining in South Africa has played and continues to play a vital role in building the country's economy for over a century and a half. The mining of bituminous coal in South Africa has served as a leading source of energy for the production of industrial and domestic electricity in the country for many years (Hancox and Götz, 2014). According to the Department of Mineral Resources and Energy (2015), 77% of South Africa's main energy source is derived from coal. During the combustion of low-grade coal for electricity generation, a large amount of coal utilisation by-products (CUP), such as coal fly ash (CFA), bottom ash, and flue-gas desulfurization gypsum, are generated. CFA is the fine, spherical particle forming part of coal ash, lighter and less dense than heavy and coarse bottom ash, and has some cementitious properties (Chou, 2012b).

The CFA, produced after combustion of the low-grade coal, is then transported out of the boiler through exhaust gas pipes through an electrostatic precipitator or bag filter system (Eskom, 2016). After the removal, most of the CFA is collected and transported to a landfill or an ash dump. According to Eskom (2016), the yearly CFA production of South Africa amounts to 25 Mt. Only ca. 10% of the yearly produced coal fly ash is recycled in building concrete, agriculture, construction, and backfilling mines (Eskom, 2016; Reynolds-Clausen and Singh, 2019; Yao et al., 2015). The majority (ca. 95%) of CUP remains unused and stowed away in landfills, ponds, and/or ash dams (Fatoba and Petrik, 2015), where they are exposed to the environmental soils and waters, namely through precipitation, surface water, groundwater, and/or runoff (Yeheyis et al., 2008). The long-term exposures to weathering of the CFA pose pressure on the surrounding environmental systems. Therefore, accurate studies of the mineralogical and chemical compositions of CFA are becoming increasingly significant, in order to identify the potential negative effects related to them.

The increased demand for energy in the country has led to high-energy prices and the increased combustion of coal for energy production, which in turn, causes the rise in production of CFA and their related environmental effects. CFA has the potential to

release toxic trace elements that can travel through the environment as fly ash dust and/or runoff, because of exposure to rain and erosion (Raja et al., 2015; Yang et al., 2020). Therefore, it is important to investigate the physical, mineralogical and chemical composition of CFA to fully understand the leaching behaviour of potentially toxic trace elements that could become bioavailable within the environment.

Studies of the physical, chemical and geotechnical properties of CFA have been recently conducted in South Africa by Matjie et al. (2005), Mishra et al. (2010), Ayanda et al. (2012), and Nyale et al. (2014). The mineralogy and geochemistry play an important role in the characterisation of the CFA, because the chemical composition of fly ash depends on the parental coal, and therefore varies from one source to another.

Various aspects contribute to the difference in the chemical composition of CFA, such as the burning procedure, the original coal characteristics, the ignition temperature levels, and the variation in the source of the coal (Kruse et al., 2013). This study focuses on assessing the chemical composition and Sr isotopes of CFA from various coal-fired power stations in South Africa. The total geochemical characterisation of the CFA samples provides insight into their potential environmental effects, and in turn, can help in finding better environmental management strategies for CFA in the future.

A proven environmental tracer for CFA is represented by the Sr isotopic compositions. Spivak-Birndorf et al. (2012) and Brubaker et al. (2013) showed the relationship between Sr isotope compositions of CFA and their potential of affecting the mobility of toxic trace elements, such as Mo, As, and V in high pH conditions, and Cu, Ni, Pb and Zn in low pH conditions. The Sr isotopic composition of CFA in South Africa is unknown, as this method has not yet been applied in South Africa. This study will therefore provide the first step into bridging the gap in knowledge of the Sr isotope composition of CFA in South Africa. The initial small dataset presented in this research lays the foundation for future studies into the leaching behaviour and mobility of Sr and toxic trace elements. The results will also allow the comparison of bulk Sr isotope compositions of CFA in South Africa with samples analysed in other studies overseas.

The enrichment of rare and heavy metals in CFA carries implications. On one side, their high concentrations may represent a risk to the environment. At the same time, this enrichment can also be assessed as potential mineral resources of these metals. In recent years, the relative enrichment in rare earth elements (REE) in CFA has been evaluated as a promising and potential alternative resource for the extraction of REY (Seredin and Dai, 2012; Seredin et al., 2013; Wagner and Matiane, 2018; Tang et al., 2019; Mokoena et al., 2022). REE are regarded as important critical materials used in various fields such as electronics, energy, defence, and automotive industries (Taggart et al., 2016). REE consists of 15 lanthanides (Ln, Ce, Pr, Nd, Pm, Sm, Eu, Gd, Tb, Dy, Ho, Er, Tm, Yb, and Lu), yttrium (Y), and scandium (Sc), all of which are chemically similar (Mokoena et al., 2022). The increased demand for REY (REE + yttrium) has resulted in a global concern regarding supply vulnerability (Humphries, 2010). This has brought about the increased search to find alternative sources for REY, to increase their global security.

Due to the variable abundance and value of REY's in CFA, Seredin and Dai (2012) derived a classification method based on relative demand in the industry. The REY's are classified into three economic clusters, namely:

- Critical = Nd, Eu, Tb, Dy, Y, and Er
- Uncritical = La, Pr, Sm, and Gd
- Excessive = Ce, Ho, Tm, Yb, and Lu

Elements such as La, Ce, Pr, Nd, and Sm are geochemically classified as light REE (LREE), Eu, Gd, Tb, Dy, Y are classified as medium REE (MREE), and Ho, Er, Tm, Yb, Lu are classified as heavy REE (HREE) (An, 2014).

The extraction of REE from CFA has proven to have numerous advantages. Firstly, the availability of CFA provides a strong environmental incentive, and reusing the waste product can be beneficial (Taggart et al., 2016). Secondly, extensive excavation would not be needed to obtain the CFA, removing the possibility of using an environmentally destructive method (e.g. REE mining) to obtain REE (Taggart et al., 2016). Lastly, several costly ore processing steps can be eliminated due to the fine powder of the CFA that makes it ideal for processing (Taggart et al., 2016).

1.2 Aims and Objectives

The main aim of this study is to report on the mineralogy, geochemistry, and Sr isotopic characteristics of CFA from five distinct Eskom coal-fired power stations from the Mpumalanga Province of South Africa.

The results will be examined to address the following research questions:

1. Which minerals are detected within the CFA samples?
2. In which classification class do the CFA samples fall?
3. What are the major and trace chemical compositions of the coal fly ash?
4. In comparison to other studies on coal fly ash, is the chemical composition similar or different?
5. What is the Sr isotopic composition of the coal fly ash? How does it compare with studies from overseas?
6. Do the studied coal fly ash samples qualify as a potential source for rare earth element (REE) extraction?

Determining the high-quality trace elements and isotopic data is paramount for a reliable and accurate environmental analysis of the potential toxicity of the CFA in the area neighbouring coal-fired power stations. The provenance of CFA samples from five distinctive power stations allows the comparison of the mineralogical, geochemical and Sr isotopic compositions amongst the samples in South Africa, and those described internationally. Furthermore, the obtained high-quality trace elements data allows the evaluation of the potential recycling of these CFA samples as a resource for rare, heavy, and critical metals, such as REE.

CHAPTER 2 – Literature Review

Traditionally, most of the research associated with the effects of CUP on soil and water focused on the affinity of trace elements with inorganic Fe-sulphides (pyrite) present within the coal (e.g. Silva et al., 2011; Chou, 2012a; Bell et al., 2001). More recent studies, however, highlighted the presence of a significant amount of trace elements and metals also associated with silicate minerals (e.g., Akinyemi et al., 2020). Major elements, such as Al, Fe, Mg, Ca, K, and Na, as well as potentially leachable toxic trace elements, namely Hg, As, Se, Ni, B, Zn, Cr, V, Sr, and Pb, have the potential of being released from the coal utilisation by-products into environmental soils and waters (Querol et al., 1995; Izquierdo and Querol, 2012). The parent coal plays a large role in the potential mobility of an element from CFA into the environment (Izquierdo and Querol, 2012).

Izquierdo and Querol (2012) reviewed an assemblage of publications focused on CFA worldwide and discovered general trends in the leaching behaviour of CFA that the investigated CFA in this study may also follow. The literature review found there to be low solubility of Be, Cd, Co, Cu, Fe, Mg, Mn, Ni, Pb, REE, Si, Sn, Th, Tl, U, and Zn in pH ranges between 7 and 10, which is in contrast to the oxyanion-forming species (As, B, Cr, Mo, Sb, Se, V, and W) that achieved maximum leachability within the same pH ranges (Izquierdo and Querol, 2012). The main species of concern were As, B, Cr, Mo, and Se due to their elevated solubility and mobility into ground and surface water. Gopinathan et al. (2022) conducted a study into the geochemical, mineralogical, and toxicological characteristics of CFA and their subsequent environmental effects. Crystalline and amorphous materials were found within the nano minerals of the CFA, suggesting that the nano minerals were highly aggregated in the CFA (Gopinathan et al., 2022). Although the CFA comprised primarily of Si-based minerals, potentially dangerous elements, namely Cd, Co, Cr, Pb, Se, V, Sn, Cu, and S, were found within the nano minerals (Gopinathan et al., 2022). Unburnt carbon was also detected within the CFA samples (Gopinthan et al., 2022). The study revealed CFA to be non-toxic in low concentrations however, in higher concentrations it can be a source of toxicity to the environment surrounding a coal power station (Gopanathan et al., 2022).

2.1 Previous chemical studies on coal fly ashes in South Africa

Environmental analysis of the geochemical fractionation of fresh and weathered CFA in South African coal-fired power stations have previously been conducted by Akinyemi et al. (2012; 2020), Ayanda et al. (2012), Van der Merwe et al. (2014) and Nyale et al. (2014). A comparative study into the geochemical fractionation of hazardous elements between weathered and fresh CFA samples was conducted by Akinyemi et al. (2020). The study focused on understanding the migration, redistribution, and mineral transformation of chemical species in CFA that encountered environmental waters, oxygen, and carbon dioxide (Akinyemi et al., 2020). The results showed a distinction between the weathered and fresh CFA. A relative enrichment in amorphous glass was observed in the weathered CFA in comparison to the fresh CFA, which is suggestive of a higher reactivity within the weathered CFA (Akinyemi et al., 2020). The weathered and fresh CFA also had differences in their enrichment of minerals. The weathered CFA shows enrichment in ettringite, inertinite, maghemite, and mullite (Akinyemi et al., 2020). In comparison, the fresh CFA shows a moderate enrichment in Al-Fe-oxides, calcite, and tridymite (Akinyemi et al., 2020). Somewhat similarly, Alegbe et al. (2018) found the mineralogical characteristics of the CFA collected at the Hendrina, Matla, Kriel, Secunda, and Tutuka Power Stations to contain calcite, hematite, gypsum, magnetite, mullite and quartz. Van der Merwe et al. (2014) identified mullite, and quartz as the main crystalline phases found in the CFA sourced from an undisclosed South African power station.

The percolation of pore water pH through the weathered CFA resulted in the mobilisation of soluble oxides, namely CaO, K_2O, and Na_2O, out of the CFA, leading to the depletion of soluble oxides within the weathered CFA (Akinyemi et al., 2020). The pH of leachate was found to play a major role in the mobilisation of major and minor elements in studies conducted by Fatoba (2008), Gitari et al. (2009), and Mbugua (2012). The calculated mobility factor revealed high mobility and leaching of elements such as K, Sr, V, Cr, Cu, Se, and B in the weathered CFA and Ca, Se, Na, Mg, Mo, and Sb in the fresh CFA (Akinyemi et al., 2020). Gitari et al. (2009) discovered minor elements such as As, B, Fe, Mn, and Se to be released into the environment in low pH conditions ranging between 10 and 4. Consistent with the findings of Akinyemi et al. (2020) are the results of the studies of Akinyemi et al. (2012) and Nyale et al. (2014). Akinyemi et al. (2012) and Nyale et al. (2014) showed that the gradual

reduction of pore water pH, ash interaction chemistry, and ash sampling point (i.e. compaction due to overburden) are factors that control the trends in depletion and enrichment of the major elements in the CFA. Nyale et al. (2014) discovered that trace elements such as As, Cu, Cr, Mo, Pb, and Zn are readily leached from labile phases over time. Akinyemi et al. (2012) also discovered that the weathered hydraulically disposed CFA is not a sustainable salt sink due to the occurrence of the leaching and migration of Na+ and K+.

Gitari (2006) investigated and evaluated the leachate chemistry and contaminants attenuation concerning acid mine drainage by fly ash, similar to a study by Vadapalli et al. (2008) who investigated the neutralization of AMD through the use of CFA. The first part of the study involved the evaluation of the neutralization capabilities of CFA when exposed to AMD, as well as the CFA's removal capacity of inorganic contaminants (Gitari, 2006). It was determined that the final pH in the reaction mixture as well as the amount of FA within the mixture are directly linked to the efficiency of elemental removal of AMD by the FA (Gitari, 2006), similar to the findings made by Akinyemi et al. (2012, 2020) and Nyale et al. (2014). Upon exposing CFA to AMD, Vadapalli et al. (2008) observed an immediate increase in pH and a decrease in electrical conductivity. The next part of the study by Gitari (2009) focused on examining FA's removal capacity of inorganic components from AMD through time. Geochemical modelling software was used to determine this and it was discovered that at ratios of 1:3 and 1:1.5 FA: AMD, there was a saturation or oversaturation of the reaction mixture with various minerals (i.e. alunite, basaluminite, boehmite, gibbsite, etc.) at specific contact times (Gitari, 2006). Vadapalli et al. (2008) removed a high percentage of major and minor elements, as well as SO_4^{2-}, through the addition of CFA to the AMD solution. In the third and final part of the study, a column leaching test was conducted on the solid residue that was blended with varying amounts of FA (i.e. 5%, 25%, and 40%) and 6% Ordinary Portland Cement (OPC) to evaluate the contaminant attenuation with time. The main determining factor for contaminant attenuation was discovered to be pH (Gitari, 2006), similar to the findings of Vadapalli et al. (2008).

Musyoka (2009) studied Class F South African CFA with a focus on obtaining pure-phase zeolite Na-P1 through optimizing synthesis conditions. The most suitable condition to achieve this was under relatively mild temperature conditions. After using

a systematic approach, which included a statistically designed experiment to understand the distinct variation in phase purity due to synthesis conditions, it was discovered that toxic elements could effectively be removed from brine through zeolite Na-P1 synthesizing with a high cation exchange capacity (Musyoka, 2009).

Recent studies have focussed on maximizing the value chain of coal-burning by-products from South Africa and the potential use of CFA for novel applications, in line with the concept of industrial ecology and the circular economy (Fernandes et al., 2021).

2.2 Chemical and Sr isotopic compositions of coal fly ashes: case studies from overseas

The use of mineralogy, geochemistry, and Sr isotope systematics for the characterisation of soils and coal fly ash in environmental studies has been applied in North America for a long time (e.g. Mattigod et al., 1990; Spivak-Birndorf et al., 2012). Strontium isotopic data on environmental waters has also been used in the characterisation of water-rock interactions, to track fluid flow and to fingerprint the nature of the contamination sources (Brubaker et al., 2013).

Strontium (Sr), one of the trace elements associated with ash produced by coal, has 4 naturally occurring isotopes, namely ^{84}Sr, ^{86}Sr, ^{87}Sr, ^{88}Sr, all of which are stable (Faure, 1977). Mattigod et al. (1990) showed a correlation between an increasingly higher ratio of $^{87}Sr/^{86}Sr$ and the ash produced by higher-rank feed coals, such as sub-bituminous and bituminous coal, in comparison to the slight correlation of the $^{87}Sr/^{86}Sr$ ratio with the ash produced in lower-ranked coal, such as lignite. According to Hurst et al. (1991), the Sr isotopes in CUP are comparatively more enriched than they are in coal and are readily available for mobilization. Therefore Sr isotope data has been used as a tool to understand the interaction between CUP and meteoric water (e.g., Spivak-Birndorf et al., 2012; Brubaker et al., 2013).

Radiogenic Sr isotope ratios ($^{87}Sr/^{86}Sr$) have long been used as tracers of fluids and water-rock interactions within geological and environmental systems (Capo et al., 1998). They can help in identifying different phases in CUP that may potentially carry

toxic trace elements (Spivak-Birndorf et al., 2012). It is a sensitive technique and it can also assist in tracking the release of toxic trace elements into the environment (Spivak-Birndorf et al., 2012).

The β decay of rubidium (^{87}Rb) usually results in the increased concentration of Sr isotopes within geological materials over long periods (Spivak-Birndorf et al., 2012). The different variations in Sr isotope ratios within these materials reflect the difference in age as well as long-term Rb/Sr ratios. These variations can therefore be used to uniquely identify and quantify their involvement in environmental and geological processes. In this study the Sr isotope compositions are reported as ε_{Sr}^{SW} values, which is the sample ^{87}Sr/^{86}Sr ratio normalized to the present-day seawater ^{87}Sr/^{86}Sr ratio:

$$\varepsilon_{Sr}^{SW} = 10^4 \left(\frac{^{87}Sr/^{86}Sr_{sample}}{^{87}Sr/^{86}Sr_{seawater}} - 1 \right)$$

The variations in ε_{Sr}^{SW} are used as a method of identification of the Sr sources in coal-related systems (Brubaker et al., 2013).

2.3 Potential extraction of REE from CFA studies in South Africa

South Africa has a considerably large coal reserve, on which the country at the moment is relying for the production of electricity. The elevated consumption of coal is reflected in the significant amount of CFA produced. The high tonnage of produced CFA, together with problems related to its storage, has led to studies on the potential re-use of CFA and their assessment as potential mineral resources (e.g. Matjie et al., 2005, Wagner and Matiane, 2018). In addition to the common recycling of CFA for construction materials and backfilling in mines, Wagner and Matiane (2018) investigated the potential use of CFA for REE (rare earth elements) extraction. Matjie et al. (2005) explored the use of CFA for the extraction of alumina and Fernandes et al. (2021) focused on the use of CFA as a potential oxygen reduction reaction in electrocatalysts.

The increased global demand of REY and critical metal resources, due to their application in alternative renewable energy production, has seen the evaluation of

REY occurrences in South African coal (Wagner and Matiane, 2018) and CFA (Wagner and Matiane, 2018; Mokoena et al., 2022). Wagner and Matiane (2018) studied the relative enrichment REY + Sc in CFA from three Main Karoo Basin (MKB) South African power station feed coals. The samples consisted primarily of an amorphous glassy phase, with glassy cenospheres, ferrospheres, and quartz (Wagner and Matiane, 2018). The study found the REY concentrations of the coal samples to range between 95 and 149 ppm, while the REY concentration in the CFA samples ranged between 402 and 599 ppm (Wagner and Matiane, 2018). The REY concentrations of the CFA were 1.5 to 3 times higher than the average upper continental crust (UCC) values but lower than the REY-rich coal ashes recorded for various deposits globally (Wagner and Matiane, 2018). Wagner and Matiane (2018) also found the CFA not to be enriched in the six critical REY + Sc elements for magnets (Nd, Pr, Dy, and Tb) and phosphor (Eu, Tb, and Y).

Although the study found the CFA to be a promising source for REY + Sc extraction based on the outlook coefficient of REY set out by Seredin and Dai (2012), Wagner and Matiane (2018) discovered that the CFA that's derived from the MKB power station feed coals does not qualify as a potential source according to the updated evaluation plot set out by Dai et al. (2017). The potential significant recovery of REE from South African CFA is also not supported by Mokoena et al. (2022). This study focused on the effects of acid concentrates on the recovery of REE using CFA from the Tutuka coal-fired power station. Although the alkali fusion-acid leaching method was significantly effective in extracting and recovering REE from the CFA, the total REE extracted and recovered was low (Mokoena et al., 2022). The alkali fusion-acid leaching method dissolved REE-bearing minerals (quartz, mullite, allanite rutile, etc), but it did not dissolve other acid-resistant phases (Mokoena et al., 2022). This method favours the recovery and extraction of MREE and HREE over LREE but yields a low recovery in the total REE (Mokoena et al., 2022). The geometallurgical processing necessary for recovery and extraction of REE from CFA is beyond the scope of the Mokoena et al. (2022) study however, the study shows the importance of accurate characterisation of the mineralogical assemblages constituting the CFA, which may be very variable and can change from one power station to another.

2.4 Potential extraction of REE from CFA in other countries

Pan et al. (2018) conducted a case study on the modes of occurrence of REE in CFA found in the Guizhou Province, China. The study by Pan et al. (2018) revealed five types of REE occurrences in varying proportions, namely silicate-aluminate, organic or sulphide, acid-soluble, metal oxides, and ion-exchangeable form. Silicate-aluminate was the most dominant REY occurrence in the CFA (Pan et al., 2018). The REY in the CFA is more closely bound to Al/P than Si, indicating less of a correlation between Si and REY, and indicating that Al is more important for REE in comparison to aluminosilicates (Pan et al., 2018).

Taggart et al. (2016) sought to characterise the United States of America CFA with the objection of ranking their potential for REE recovery. The CFA samples were sourced from mines located in three basins within the United States of America that account for 70% - 80% of the total coal production, namely: The Appalachian Basin, The Illinois Basin, and The Powder River Basin (Taggart et al., 2016). The REE content of the Appalachian Basin CFA was 591 mg kg^{-1}, which is significantly greater than the 403 mg kg^{-1} and 337 mg kg^{-1} of the Illinois and Powder River Basins, respectively (Taggart et al., 2016). Compared to conventional ores, the fraction of the critical REE in the studied CFA's was 34 – 38%, a value greater than the less than 15% typically found in conventional ores (Taggart et al., 2016). Taggart et al. (2016) also attempted to study the extractability and recovery of REE from the CFA using the heated nitric acid digestion method. This method proved to be effective in recovering 70 % of the total REE from the Powder River Basin CFA, (the basin with the lowest REE content) than in the Illinois and Appalachian Basins where less than 3% of the total REE was recovered for both CFA samples. This was attributed to the high Ca content (eg. Class C CFA) found within the Powder River Basin CFA that caused a greater fraction of the CFA particles to dissolve during the nitric acid extraction process, exposing more surface area that resulted in the release of REE from the fly ash matrix (Taggart et al., 2016). Therefore, CFA with high Ca content exhibits sufficiently higher extraction efficiencies when utilising the heated nitric acid digestion method (Taggart et al., 2016). Taggart et al. (2016) concluded that new REE recovery technologies will need to be developed that are specifically tailored to various types of CFA to achieve scalable, high-efficiency recovery in order to take advantage of the high REE content that was identified in the Appalachian Basin CFA.

Tang et al. (2019) investigated the effects of using a two-step hydrometallurgical process (alkali fusion-acid leaching) compared to the low recovery, direct leaching method commonly used to extract and recover REE from CFA. The results indicated a higher leaching efficiency of REE by using the alkali fusion-acid leaching method compared to the direct leaching method (Tang et al., 2019). The REE extraction process is slow, taking a relatively long time to achieve leaching balance when using the direct leaching method (Tang et al., 2019). The optimum conditions for fusion treatment were achieved by obtaining a mass ratio of 1:1 for the CFA/Na_2CO_3 heated to a temperature of 860°C for 0.5 hours (Tang et al., 2019). This led to the achievement of an REE leaching rate of 58.38% after 120 minutes (Tang et al., 2019). To achieve optimum leaching conditions, a stirring speed of 400r/min with a concentration of 3 mol/L of the HCl and a 1:20 solid-liquid ratio, was used to achieve a REE leaching rate of up to 72.78% (Tang et al., 2019).

CHAPTER 3 – Methodology

3.1 Sample selection

This study focuses on five samples of coal fly ash (CFA) from diverse Eskom-owned coal-fired power stations in South Africa (Figure 1). Coal fly ash samples from the Tutuka and Kriel Power Stations were obtained from Professor Sehliselo Ndlovu from the School of Chemical and Metallurgical Engineering, University of the Witwatersrand. The samples from the Grootvlei and Hendrina Power Stations were obtained from Prof. Nikki Wagner, Department of Geology, University of Johannesburg. The fifth CFA sample from Komati Power Station was obtained from Dr. Sehai Mokhahlane, School of Chemical and Metallurgical Engineering, University of the Witwatersrand. The samples were not processed at the time of acquisition.

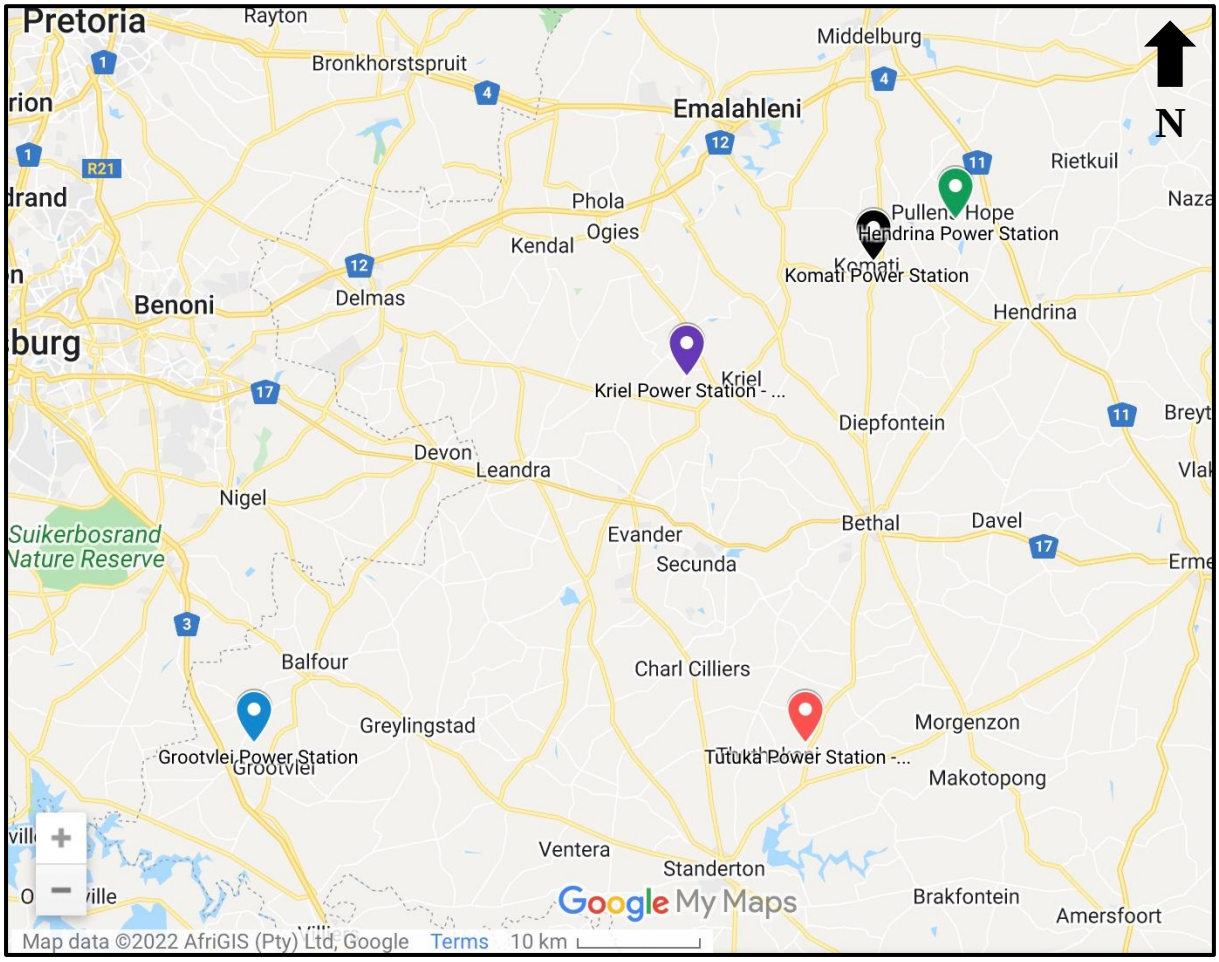


Figure 1: The CFA samples focus of this study were obtained from five different coal-fired power stations in the Mpumalanga Province of South Africa.

3.2 Powder X-Ray Diffractometry (PXRD)

The major crystalline phases of the Grootvlei, Hendrina, and Komati coal fly ash samples were analysed using a Brucker D2 Phaser powder X-ray diffractometer (PXRD, Figure 2) equipped with a cobalt radiation source and a Lynxeye detector, housed in the School of Chemistry, University of the Witwatersrand. Tutuka and Kriel's samples were previously analysed by XRA Analytical and Consulting, South Africa.

The PXRD analysis was performed at room temperature and the coal fly ash sample powders were placed inside the sample holder. The measurements for the Grootvlei and Hendrina coal fly ash samples were done at peak intensities of $10<2\theta\leq90$ for 60 minutes with no spin, while the Komati coal fly ash sample was done at peak intensities of $5<2\theta\leq90$ for 60 minutes with no spin. The first peak for the Komati sample was detected at ca. 11 two theta (2θ).

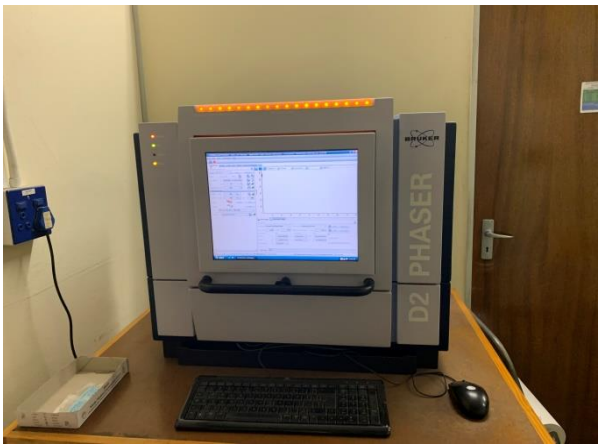


Figure 2: The Brucker D2 Phaser Powder X-Ray Diffractometer (PXRD) at The School of Chemistry, University of the Witwatersrand

PXRD analysis of samples from Tutuka and Kriel powers station were independently obtained from Prof. Ndlovu from the School of Metallurgy, University of the Witwatersrand. The analyses were conducted using the back-loading preparation method. A Malvern Pananalytical Aeris diffractometer with PIXcel detector and fixed slits with Fe filtered Co-Kα radiation was used to identify the major crystalline phases. The X'Pert Highscore Plus software was used to identify the mineralogy of the Tutuka and Kriel coal fly ash samples.

3.3 X-Ray Fluorescence (XRF) Analysis

The major element analysis of the Grootvlei, Hendrina, and Komati CFA samples was performed at the Earth Lab, University of the Witwatersrand. The Norrish Fusion technique (Norrish and Hutton) was used to determine the major elements using a Pananalytical Axios X-Ray Fluorescence Spectrometer. Approximately 2.0 g of flux was added to 0.35 g of sample powder and the mixture was fused using Johnson Matthey Spectrolflux 105 at 1000°C. The in-house software was then used offline to correct the major elements' raw data. The instrumental standard calibration was obtained using synthetic oxide mixtures and international rock reference materials that were prepared in-house from the USGS series (USA) and NIM series (South Africa), such as BCR2, BHVO2, and AGV2 (Table 1). For elements that occurred in abundances greater than 5% by weight, the precision was taken as 1%. Elements that occurred in abundances less than 5% were taken at a precision of 5%.

Table 1: Comparison of the measured and recommended values for international rock reference material from the USGS in %

	BCR2 measured	BHVO2 measured	AGV2 measured	BCR2 Recom.	BHVO2 Recom.	AGV2 Recom,
SiO_2	54.80	50.38	60.65	54.06	49.9	59.30
Al_2O_3	13.63	13.73	17.31	13.40	13.75	17.03
Fe_2O_3	1.40	1.25	0.68	--	--	--
FeO	11.31	10.15	5.53	12.45	9.41	5.96
MnO	0.19	0.16	0.10	0.20	0.17	0.10
MgO	3.63	7.32	1.84	3.55	7.24	1.79
CaO	7.19	11.48	5.31	7.18	11.49	5.15
Na_2O	3.19	2.23	4.28	3.11	2.21	4.20
K_2O	1.79	0.52	2.94	1.78	0.52	2.89
TiO_2	2.28	2.76	1.06	2.27	2.73	1.05
P_2O_5	0.35	0.27	0.48	0.35	0.27	0.48
Cr_2O_3	0.02	0.06	0.01	--	--	--
NiO	0.00	0.02	0.00	--	--	--
LOI	0.10	-0.48	1.80	--	--	--
TOTAL	99.77	100.31	100.19	--	--	--

Recom = recommended values from GeoReM
LOI loss-on-ignition at 1050 °C

Major elements for the Tutuka and Kriel samples were previously independently determined by UIS Analytical Services (Pty) Ltd in Centurion, Gauteng using a LECO CS230 instrument.

3.4 Trace elements and REE analysis

All five CFA samples were analysed for trace elements compositions by ICP-MS data using a Thermo Scientific iCAP RQ instrument in the Earth Lab at The University of the Witwatersrand (Figure 3). The sample digestion was performed using an open beaker/hotplate method. Approximately 50mg of the CFA sample was placed into the 15ml Savillex beaker with 3ml of Ultra High Purity 2:1 HF:HNO3 and placed on the hotplate at 70°C. Once the samples were dried, an additional 3ml of HF: HNO3 was added, and the beakers were capped, and placed on the hotplate at 70°C. After about 72 hours, the beakers were opened and the mixture was allowed to dry down completely at 70°C and another 3ml HNO_3 was added and evaporated off. Then, a further 3ml HNO3 was added and the beaker was capped and placed on the hotplate at 70°C. After 24 hours, the beakers are opened and once the acid was evaporated, another 3 ml of HNO_3 was added again and the sample was subsequently dried. In the final step, the samples were re-dissolved and stored in 300µl HNO_3 until they were ready to be analysed for trace elements in the Thermo Scientific iCAP RQ (Figure 3).

Before the analyses were undertaken, the samples (stored in 300µl HNO_3) were further diluted using 5% HNO_3 in analytical vials, to 50ml (dilution factor of 1:1000). At the same time, each sample was spiked with an Internal Standards, 100ppb of Re and Rh and 50ppb of In and Bi, in order to monitor the quality of the analytical work throughout the session. Before the analysis, each sample vial was visually inspected for fluorides, which may occur as solid precipitate at the bottom of the vial. During the analytical session internal calibration standards, which were made in-house in different concentrations (10, 30, 50, 75, and 100pbb), together with International Certified Reference Materials, such as BCR-2, BHVO-2, and BIR-1, were analysed among the samples (Table 2)

Table 2: Comparison of measured and recommended values for USGS reference materials measured among the samples in ppm

	BCR2	BHVO2	BIR1	BCR2	BHVO2	BIR1
	Meas	Meas	Meas	Recom	Recom	Recom
Li	10.3	4.8	3.5	9.9	5.0	3.4
P	1569.8	1178.9	86.5	1571.0	1178.0	100.0
Sc	32.0	31.0	40.8	32.0	31.0	44.0
Ti	13000.6	15626.3	5555.2	13005.0	15621.0	5755.0
V	416.5	327.1	326.0	414.0	329.0	313.0
Cr	16.3	297.9	416.0	17.0	285.0	382.0
Co	37.7	44.7	53.5	35.8	47.0	51.4
Ni	11.8	121.7	176.3	12.7	112.0	166.0
Cu	18.6	148.5	139.6	19.4	142.0	126.0
Zn	142.0	110.9	76.2	147.0	107.0	71.0
Ga	22.6	21.1	13.8	22.7	21.0	--
As	0.6	0.5	0.1	0.65	0.4	0.4
Rb	50.3	9.8	0.2	49.0	10.1	0.3
Sr	325.4	376.9	101.4	321.0	382.0	108.0
Y	31.7	22.5	13.1	31.0	23.0	16.0
Zr	185.6	167.6	12.6	194.0	160.0	15.5
Nb	12.0	17.6	0.5	12.8	16.4	0.6
Sn	2.1	1.2	0.9	2.1	2.7	0.7
Sb	0.6	0.2	0.9	0.6	0.2	0.6
Cs	1.3	0.1	0.0	1.2	0.1	--
Ba	646.8	127.6	6.3	641.0	128.7	--
La	25.4	15.1	0.6	24.5	15.6	0.6
Ce	51.6	36.2	1.8	50.5	37.0	2.0
Pr	6.4	4.9	0.3	6.3	5.0	0.4
Nd	27.6	23.5	2.3	27.0	24.0	2.5
Sm	6.3	5.8	1.0	6.3	5.8	1.1
Eu	1.9	2.0	0.5	1.9	2.0	0.5
Gd	6.5	5.9	1.6	6.5	5.9	1.9
Tb	1.0	0.8	0.3	1.0	0.9	0.4
Dy	6.0	4.9	2.3	6.0	4.9	2.5
Ho	1.2	0.9	0.5	1.2	0.9	0.6
Er	3.3	2.3	1.5	3.3	2.3	1.7
Tm	0.5	0.3	0.2	0.5	0.3	0.3
Yb	3.3	2.0	1.6	3.2	2.0	1.7
Lu	0.5	0.3	0.2	0.5	0.3	0.3
Hf	4.8	4.3	0.5	5.0	4.1	0.6
Ta	0.7	1.0	0.1	0.8	0.9	0.0
W	0.5	0.3	0.1	0.4	0.3	0.0
Tl	0.3	0.0	b.d.	0.3	0.1	0.0
Pb	10.0	1.5	2.9	10.9	1.4	3.0
Th	5.7	1.1	0.0	5.5	1.2	0.0
U	1.8	0.4	0.0	1.7	0.4	0.0

Meas = Measured
Recom = Recommended values
b.d = below detection values

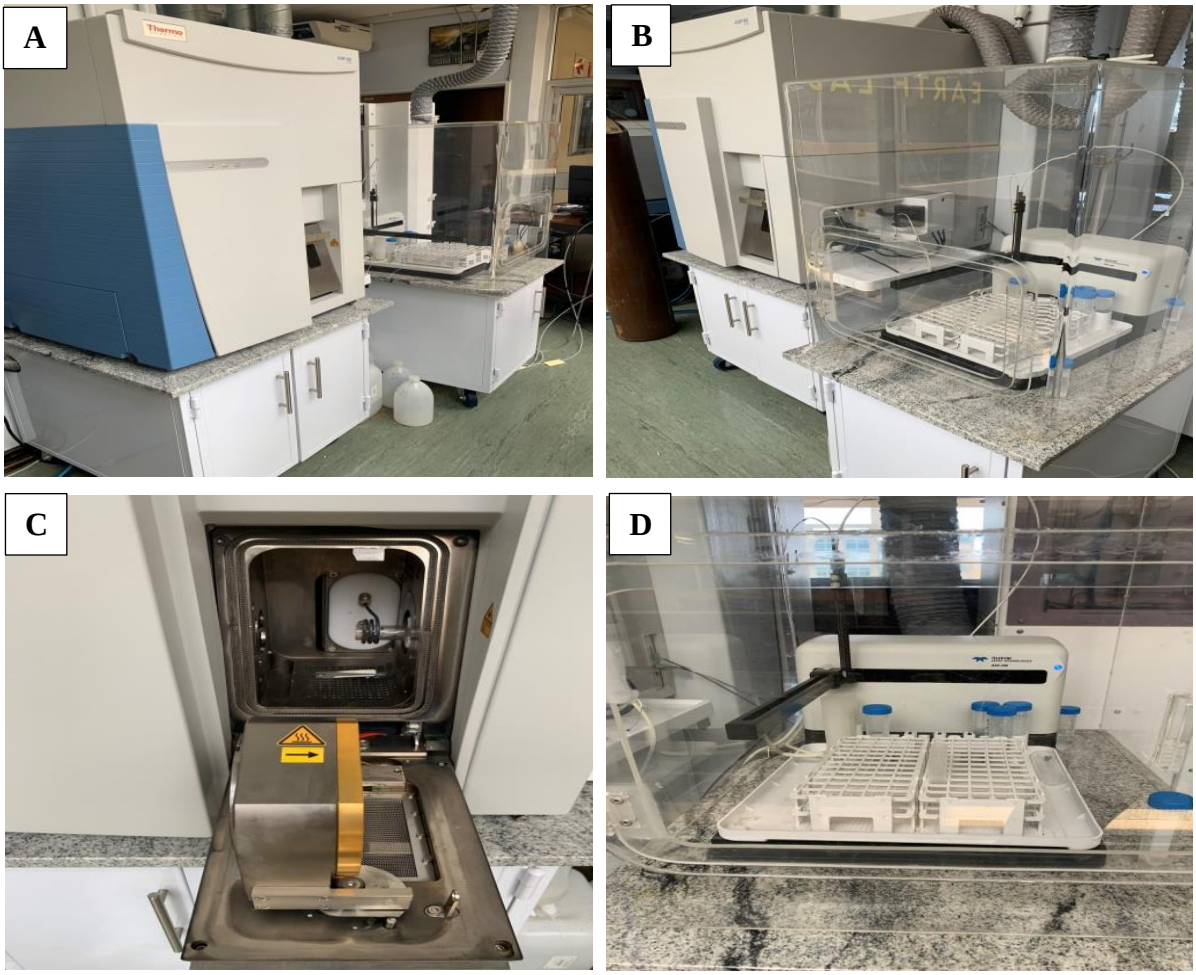


Figure 3A and B: The Thermo Scientific iCAP RQ used for the ICP-MS trace elements analysis at the Earth Lab at The University of the Witwatersrand; C) ionising chamber; D) auto sampler for the introduction of the sample solution into the ionising chamber of the iCAP.

The dissolved, diluted and spiked samples were introduced into the ionising chamber of the Thermo Scientific iCAP RQ (Figure 3C) using tubing and auto sampler (Figure 3D). The instrumental optimisation was set on less than 2% for oxides and less than 2% for doubly charged ions. Each sample was automatically analysed three times by the instrument and measurements were averaged. When the replicate deviation was greater than 2%, the analysis was flagged.

The Certified Reference Materials (CRMs) were analysed among the samples for quality control. The Reference Materials passed the Quality Controls, showing less than 10% deviation for accepted concentrations for the analysed elements (see Table 2). Among the unknown samples, a Total Procedural Blank (TPB) was also performed, in order to have an indication of the cleanness of the laboratory facility and of the

samples preparation procedure. The data obtained for the TPB was then subtracted from the raw results.

3.5 Radiogenic Strontium Isotope Analysis

The chemical separation of Rb and Sr from the matrix was performed by the author under ultra-clean conditions at the Wits Isotope Geoscience Laboratory (WIGL) at the School of Geoscience, University of the Witwatersrand.

About 10 mg of CFA powders and ca. 30 mg of reference material AGV2 were spiked with mixed Rb-Sr tracers (Table 3) and dissolved in a mixture of concentrated HF-HNO_3 in PFA beakers on the hotplate at 110°C for 5 days to break down silicates. After sample dissolution, the mixture was set on the hot plate to dry down and then re-dissolved in 3 ml 6M HCl and left to reflux on the hot plate at 110°C for 48 hours. This step was repeated a second time, to convert the dissolved elements into chlorites. Then the beakers were opened to dry down and the samples were re-dissolved in 1 ml 1.5M HCl.

Table 3: Sample weights for the CFA samples and reference material AGV2

Samples	Mg	Sr spike mg
Tutuka	10.75	44.19
Kriel	10.55	73.17
AGV2	31.80	85.91

The chemical purification of the elements Rb and Sr from the matrix was obtained by chromatography, using a novel method recently set up and calibrated by Dr Linda Iaccheri in the WIGL Laboratory. The Rb-Sr separation methodology is not yet published in a peer-review paper, and the method is detailed in Khumalo et al (in preparation). Each sample was loaded into a column filled with 2 ml resin bed of BioRad AG 50W-X8, 200-400 mesh, following the calibrated elution scheme listed in Table 4.

Table 4: The calibration elution scheme for the chemical separation and purification of Rb and Sr from the matrix elements

Equilibration	2ml	1.5M HCl
	2ml	1.5M HCl
	2ml	1.5M HCl
Load samples	1ml	1.5M HCl
Rinse	1ml	1.5M HCl
	1ml	1.5M HCl
Discard	4ml	1.5M HCl
Collect Rb	3ml	1.5M HCl
Ca clean up	11ml	1.5M HCl
Collect Sr	11ml	1.5M HCl
Wash	10ml	6M HCl
	10ml	6M HCl
	10ml	6M HCl

The International Certified Reference Materials (AGV2) were processed and analysed among the unknown samples (Table 3), to monitor and validate the reliability and reproducibility of the isotope dilution schemes of the laboratory as well as to monitor the precision and accuracy of the mass spectrometer.

The Rb-Sr isotopic analyses were performed at Spectrum, University of Johannesburg, on a Nu Instruments Plasma II MC-ICP-MS (Nu Instrument, Wrexham), using a low-resolution mode wet plasma. Plasma settings included an RF power of 1300W, a coolant gas flow of 13 L/min, an auxiliary gas flow of 0.8 L/min, and a nebuliser setting of 35 psi. Data reduction was done offline using a customised Microsoft Excel spreadsheet. For Sr measurements, the accepted $^{88}Sr/^{86}Sr$ ratio of 8.375209 was used for mass bias correction calculations, and the $^{85}Rb/^{87}Rb$ ratio of 2.59576 was used to correct for ^{87}Rb interference on ^{87}Sr. The International Sr (SRM 987: $^{87}Sr/^{86}Sr = 0.710244$) yielded an average $^{87}Sr/^{86}Sr$ of 0.710249 ± 0.000017 (2σ: n = 131). The USGS reference material AGV2 yield $^{87}Sr/^{86}Sr = 0.703934\pm 0.000022$, which is within error with the accepted value of 0.703992 (GeoReM).

The present-day seawater $^{87}Sr/^{86}Sr$ ratio of 0.709164, similar to Spivak-Birndorf et al., (2012), was used to calculate ε_{Sr}^{SW}. According to Faure and Mensing (2005), the $^{87}Sr/^{86}Sr$ ratio in seawater is uniform across the Earth's crust at any given time and as a result, it can be used as a reliable and universal normalisation ratio (Spivak-Birndorf et al., 2012). The ε_{Sr}^{SW} values, which is the sample $^{87}Sr/^{86}Sr$ ratio normalised to the present-day seawater $^{87}Sr/^{86}Sr$ ratio, was calculated using the following calculation:

$$\varepsilon_{Sr}^{SW} = 10^4 \left(\frac{^{87}Sr/^{86}Sr_{sample}}{^{87}Sr/^{86}Sr_{seawater}} - 1 \right)$$

CHAPTER 4 - Results

4.1 Powder X-Ray Diffractometry (PXRD)

The PXRD analyses reveal that the CFA samples consist of various minerals, each sample characterised by slightly different mineral assemblages (Figures 4, 5, 6, and 7). All the samples show the presence of quartz (SiO_2), hematite (Fe_2O_3), magnetite (Fe_3O_4), and mullite ($Al_6Si_2O_{13}$). Quartz is the most abundant crystalline mineral observed followed by hematite and magnetite. In contrast, the presence of ettringite ($Al_2Ca_6H_{12}O_{24}S_3$) is only observed in the CFA samples from Komati, Tutuka, and Kriel power stations (Figures 6 and 7).

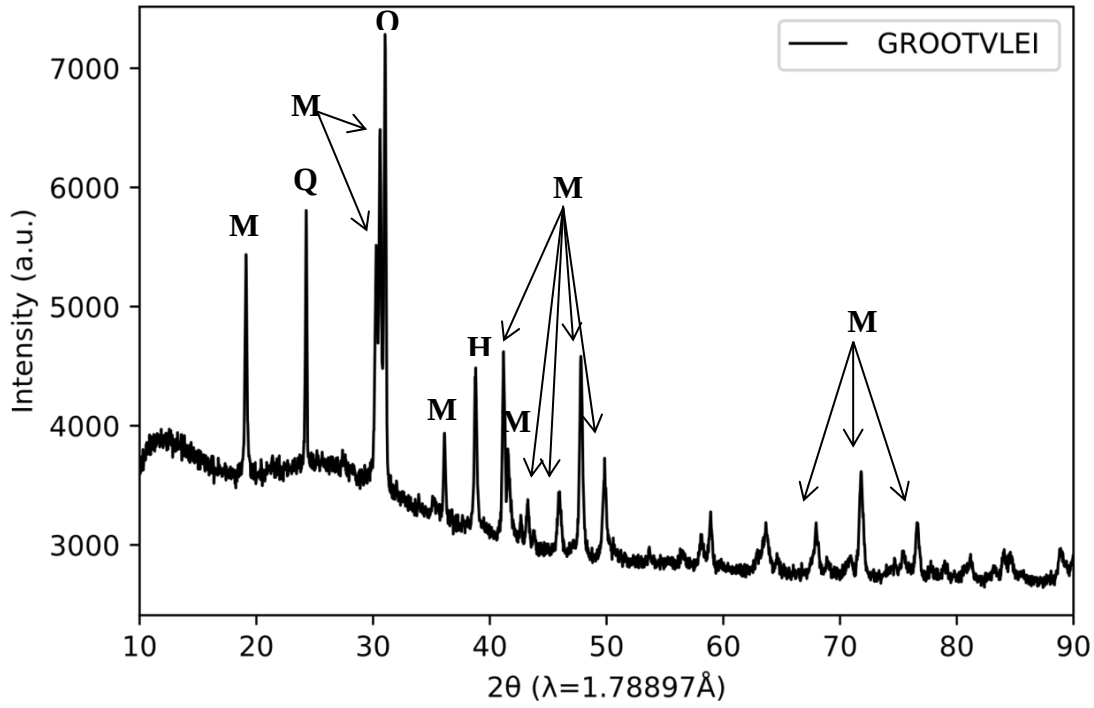


Figure 4: PXRD results for CFA from Grootvlei Power Station (M = Mullite, Q = Quartz Low, H = Hematite)

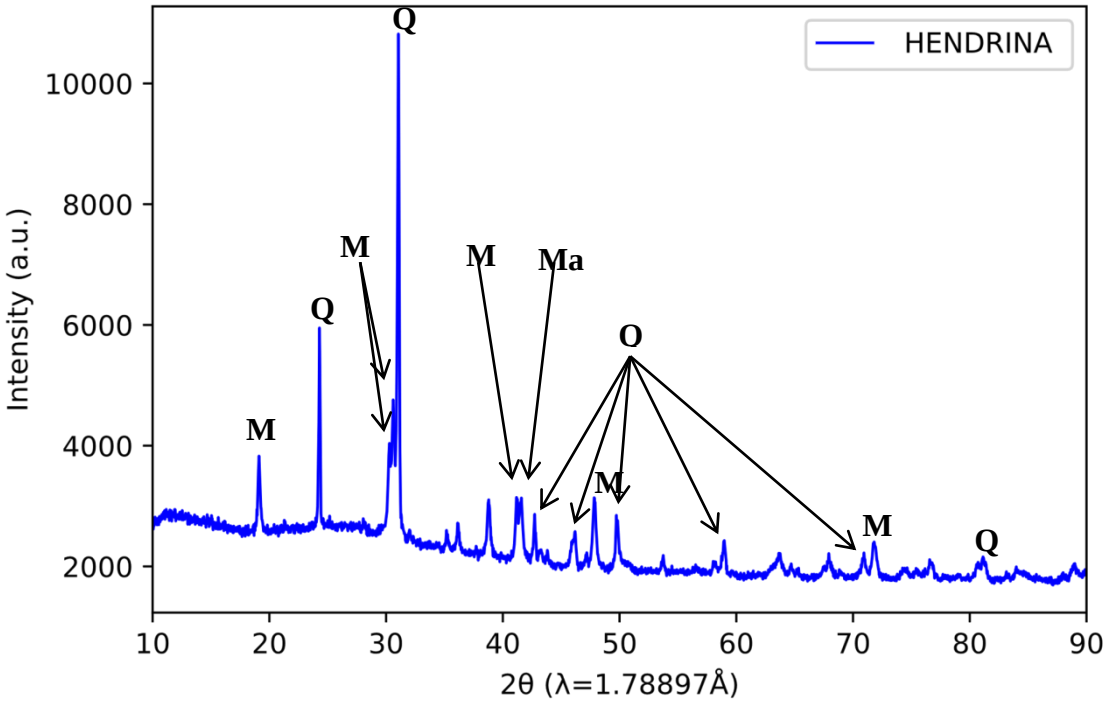


Figure 5: PXRD results for CFA from Hendrina Power Station (M = Mullite, Q = Quartz Low, H = Hematite, Ma = Magnetite)

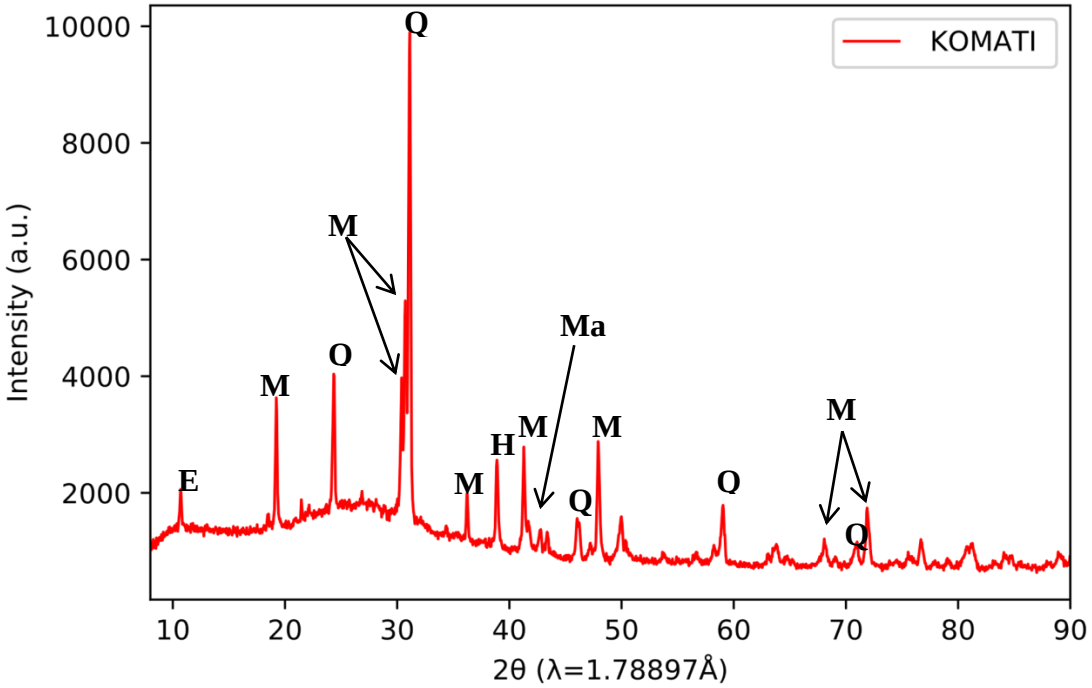


Figure 6: PXRD results for CFA from Komati Power Station (E = Ettringite, M = Muliite, Q = Quartz Low, H = Hematite, Ma = Magnetite)

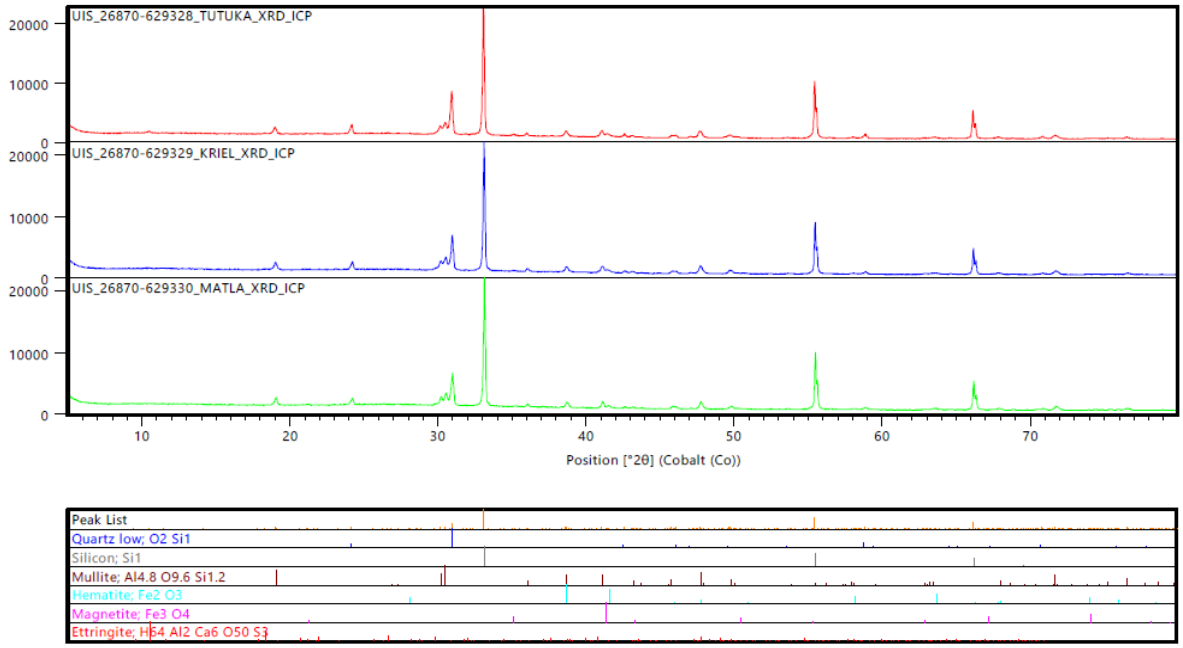


Figure 7: PXRD results for CFA from Tutuka and Kriel power stations indicating the presence of quartz, hematite, magnetite, mullite and ettringite.

4.2 Major element compositions

Major elemental concentrations of the studied CFA samples together with a representative CFA sample from Ayanda et al. (2012) are shown in Table 5. The CFA sample from the Matla coal-fired power station (Ayanda et al.2012) is reported so to compare the major elements results from this study with data from another power station in South Africa.

Table 5: Major elemental compositions (wt %) of CFA

Samples	Grootvlei	Hendrina	Komati	Tutuka	Kriel	Matla
	This study	This study	This study	Previous	Previous	Ayanda et al. 2012
SiO_2	50.54	53.35	55.28	47.50	50.50	51.43
Al_2O_3	32.24	26.82	24.78	24.40	30.20	30.93
Fe_2O_3	6.90	7.00	4.04	4.67	3.44	2.29
MnO	0.05	0.07	0.04	0.04	0.04	0.02
MgO	0.82	1.11	1.25	1.25	1.57	1.95
CaO	4.33	4.54	3.22	3.57	5.82	6.75
Na_2O	0.03	0.05	0.07	0.19	0.20	0.54
K_2O	0.74	0.55	0.60	0.69	0.99	0.77
TiO_2	1.81	1.46	1.28	1.22	1.64	1.74
P_2O_5	0.39	0.76	0.22	0.24	0.44	1.08
Cr_2O_3	0.02	0.03	0.03	0.02	0.02	0.02
NiO	0.01	0.01	0.01	0.01	0.01	0.01
LOI	1.84	3.87	9.34	3.60	2.67	1.21
Total	99.72	99.60	100.15	87.40	97.54	99.28

LOI loss-on-ignition at 1050 °C

The most abundant major element in all the samples is SiO_2, consistent with the dominant presence of quartz; followed by Al_2O_3, which is consistent with the presence of aluminium phases. There is a general similarity in the overall abundance of MnO, MgO, Na_2O, K_2O, TiO_2, P_2O_5, Cr_2O_3, and NiO. Other elements, such as Fe_2O_3 and CaO, show large variability ranging from 3.44 to 7.00 wt. % and 3.22 to 6.75 wt. %, respectively.

4.3 Trace element compositions

The trace element compositions of the CFA samples, along with the typical global Coal Clark Values used for CFA (Ketris and Yuodovich, 2009), are presented in Table 6. The trace element data has been normalised with the reported typical global Coal Clark Values in order to conduct a direct comparison with internationally accepted values (Figure 8).

The abundance of transitional trace metals and potentially toxic elements is variable among the samples. The CFA samples have relatively high values of Cr and V ranging from 148.8 to 179.1 ppm and 113.6 to 128.4 ppm, respectively. Very low

concentrations of Tl (0.6 to 1.6 ppm) were detected in all the samples, followed by relatively low concentrations of Co (14.4 to 40.3 ppm).

Compared to the Coal Clark Values CFA, all the samples analysed in this study show enrichment in Li, Ti, Cr, Ga, Sr, Nb, LREE, Ta, and Th. In contrast, all the samples show a negative correlation for P, V, Zn, Rb, Sb, HREE, Tl, and U. The base metals such as Ni, Cu, Zn, and Pb have concentrations that range between 43.4 to 95.4 ppm, 47.6 to 57.1 ppm, 34.6 to 70.8 ppm, and 49.9 to 55.5 ppm, respectively. The concentrations for Ni and Pb fall within normal ranges of the typical global values of 76 and 47 ppm, respectively, which were established by Ketris and Yudovich (2009) while the concentrations for Cu and Zn range well below the typical global values of 92 and 140 ppm, respectively (Figure 8).

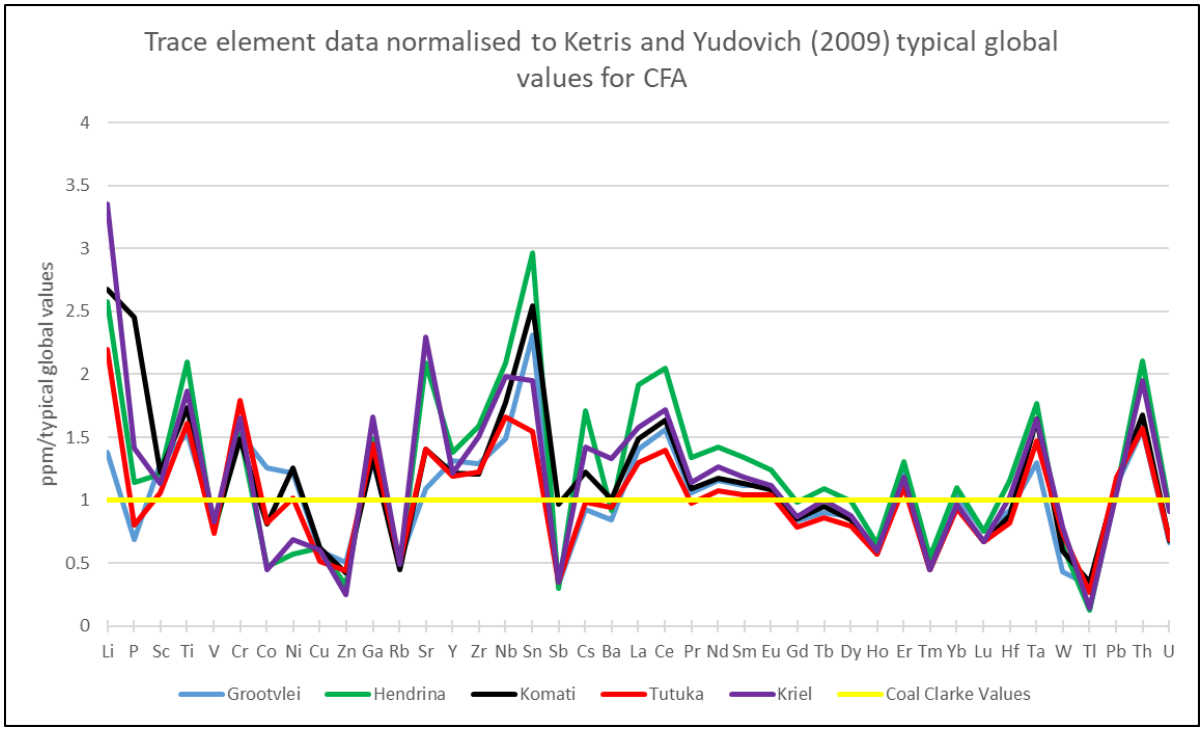


Figure 8: Graph illustrating the trace element concentrations of the CFA normalised to the typical global values for CFA by Ketris and Yudovich (2009)

The normalised REY + Sc concentrations in the Grootvlei, Hendrina, Komati, Tutuka, Kriel, and Coal Clarke Value samples exceed values typical of the Earth's upper continental crust (Figure 9). In comparison to the typical global values for Coal Clarke fly ashes determined by Ketris and Yudovich (2009), there appears to be a general similarity in the trace element concentrations, except for the CFA samples in this study

show a higher concentration in Li, Ti, Cr, Ga, Sr, Zr, Nb, Sn, La, Ce and Nd than the global values for CFA. The CFA samples also show lower concentrations of V, Cu, Zn, Rb, Sb, and Tl in comparison to the global values determined by Ketris and Yudovich (2009). Upon normalising the trace element concentrations with the typical global values (Figure 8), elements such as Li, Ti, Cr, Ga, Sr, Zr, Nb, Sn, La, Ce, and Nd rank very high above the normalised Coal Clark value of 1, indicating an enrichment in those elements, while elements such as V, Cu, Zn, Rb, Sb, Tl rank much lower than the corresponding Coal Clarke Values. Hendrina seems particularly enriched in most elements whereas Tutuka and Grootvlei generally exhibit some of the lowest values presented in Figure 8. In Table 6, it appears that all CFA samples have double the enrichment of Ti, Sr (excl. Kriel), Sn, Ce, and Li in comparison to the Coal Clarke Values. In contrast to that, the CFA samples also have less than half the enrichment of Zn, Rb, Sb (excl. Komati), and Tl in comparison to the Coal Clarke Values.

Table 6: Trace elemental compositions (ppm) of the CFA samples

Sample	Grootvlei	Hendrina	Komati	Tutuka	Kriel	Coal Clarke Values[a]
	This study	This study	This study	This study	This study	Coal fly ash
Li	91.2	170.0	176.4	144.8	221.1	66
P	928.5	1535.9	3308.6	1088.2	1912.2	1350
Sc	29.6	27.8	28.1	24.3	26.0	23
Ti	7090.1	9744.9	8077.0	7496.6	8679.8	4650
V	128.0	116.7	122.3	113.6	128.4	155
Cr	152.6	152.3	148.8	179.1	164.9	100
Co	40.3	15.0	25.9	26.3	14.4	32
Ni	92.3	43.4	95.4	77.2	52.1	76
Cu	54.8	57.1	57.1	47.6	55.5	92
Zn	70.8	44.8	59.2	62	34.6	140
Ga	43.3	49.0	44.2	47.7	54.7	33
Rb	41.0	36.8	35.2	39.9	38.7	79
Sr	810.3	1548.7	1040.7	1039.3	1697.2	740
Y	67.1	70.4	62.1	60.6	61.8	51
Zr	270.1	333.0	253.2	256.1	316.5	210
Nb	29.8	41.8	35.5	33.2	39.7	20
Sn	14.8	19.0	16.3	9.9	12.5	6.4
Sb	2.1	1.9	6.1	2.2	2.2	6.3
Cs	6.1	11.3	8.1	6.5	9.4	6.6
Ba	794.1	860.8	951.6	887	1251.4	940
La	97.2	132.3	102.9	89.7	109.1	69
Ce	202.9	265.9	212.8	181.8	223.9	130
Pr	21.1	26.7	21.8	19.5	22.8	20
Nd	77.3	95.3	78.5	72.2	84.8	67
Sm	14.5	17.4	14.7	13.5	15.4	13
Eu	2.8	3.1	2.7	2.6	2.8	2.5
Gd	13.4	15.7	13.6	12.6	13.9	16
Tb	1.9	2.3	2.0	1.8	2.1	2.1
Dy	12.1	13.9	11.8	11.1	12.3	14
Ho	2.4	2.6	2.3	2.3	2.4	4.0
Er	6.7	7.2	6.3	6.1	6.5	5.5
Tm	1.0	1.1	0.9	0.9	0.9	2.0
Yb	6.4	6.8	5.9	5.8	6.0	6.2
Lu	0.9	0.9	0.8	0.8	0.8	1.2
Hf	7.6	9.6	7.3	6.8	8.5	8.3
Ta	2.2	3.0	2.8	2.5	2.8	1.7
W	3.0	4.4	4.1	5.1	5.4	6.9
Tl	1.6	0.6	1.7	1.3	0.7	4.9
Pb	52.9	51.0	53.1	55.5	49.9	47
Th	32.8	44.2	35.2	33	40.9	21
U	10.6	15.0	10.9	11	14.6	16

[a]Ketris and Yudovich (2009)

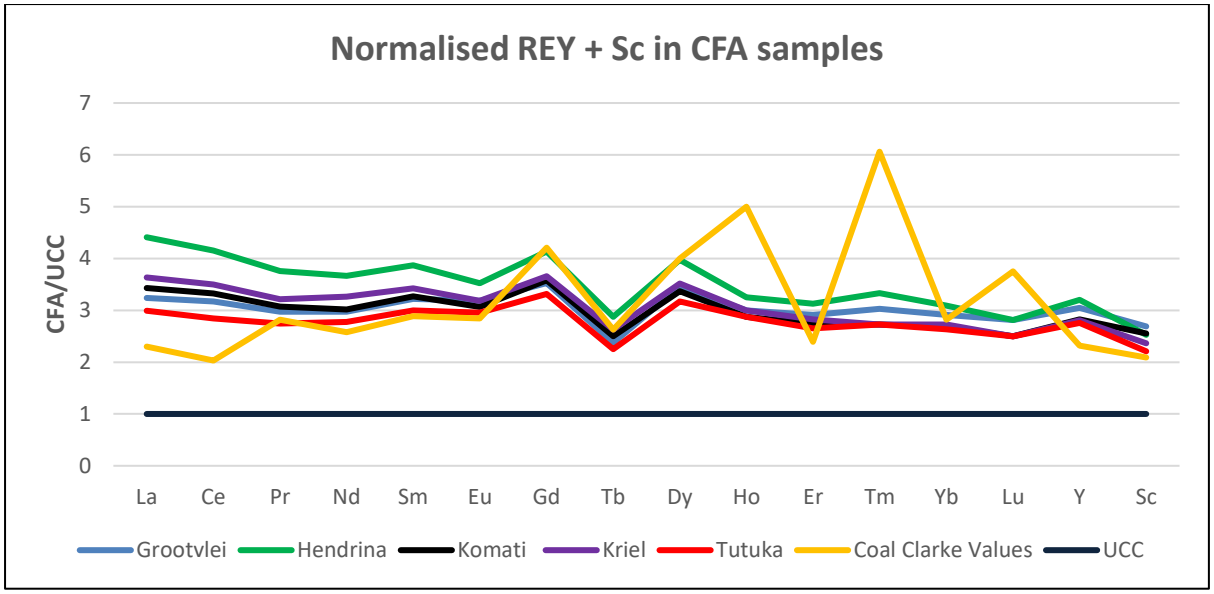


Figure 9: Upper continental crust (UCC) normalised UCC REY + Sc values of the Grootvlei, Hendrina, Komati, Tutuka, Kriel and Coal Clarke Value samples (UCC data from Taylor and McLennan, 1985. Coal Clark Values from Ketris and Yudovich (2009)

4.4 Rare earth elements concentrations

Despite the different provenance of the CFA samples analysed in this study, and potential differences in the trace element characteristics of the parental coals, all the samples show comparable REY + Sc concentrations (Figure 10).

The concentration of Ce is relatively high in comparison to other REE concentrations for all CFA samples. La, Nd, Y, and Sc have moderately high concentrations, while low concentrations of Pr, Sm, Eu, Gd, Tb, Dy, Ho, Er, Tm, Yb, and Lu are observed. Therefore, the samples show a relative enrichment in LREE and very low concentrations for MREE and HREE (Figure 10).

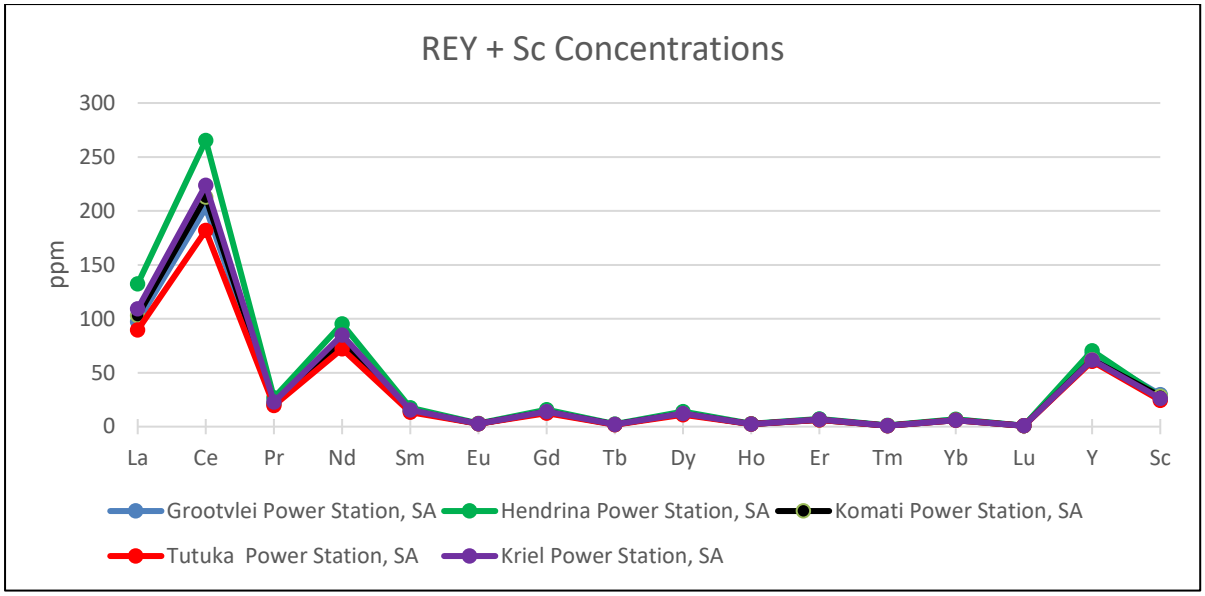


Figure 10: Concentrations of REY + Sc in the CFA of South African coal-fired power stations, arranged from light to heavy lathanides followed by Y and Sc in ppm

4.5 Strontium isotopic compositions

The Sr isotopic compositions for the CFA samples from Tutuka and Kriel power stations are shown in Table 7 and Figure 11. The data are conventionally reported relative to the present-day seawater due to the seawater Sr ratio being uniform across all oceans (Faure and Mensing, 2005), making it a suitable universal normalization ratio.

Table 7: Results 87Sr/86Sr ratios for CFA samples

Samples	Sr ppm	Rb ppm	$^{87}Rb/^{86}Sr$	$^{87}Sr/^{86}Sr$ today	1SE	ε_{Sr}^{SW}
Tutuka	985.96	37.85	0.1112	0.717859	0.000004	123
Kriel	1734.99	43.53	0.0727	0.724190	0.000004	212

The present-day seawater $^{87}Sr/^{86}Sr$ ratio of 0.709164, similar to Spivak-Birndorf et al., (2012), was used to calculate ε_{Sr}^{SW}

The lower Sr concentrations in the sample from the Tutuka power station compared to the Kriel sample (Table 7) are also reflected in its considerably lower Sr isotopic composition (Figure 10). Kriel CFA sample has radiogenic $^{87}Sr/^{86}Sr$ ratios (0.724190), while the Tutuka CFA sample has a lower $^{87}Sr/^{86}Sr$ ratio of 0.717859. Despite the only two data points, a direct correlation can be seen between εSr and $^{87}Sr/^{86}Sr$ ratio, as low $^{87}Sr/^{86}Sr$ values will result in low εSr values and vice versa (Figure 11).

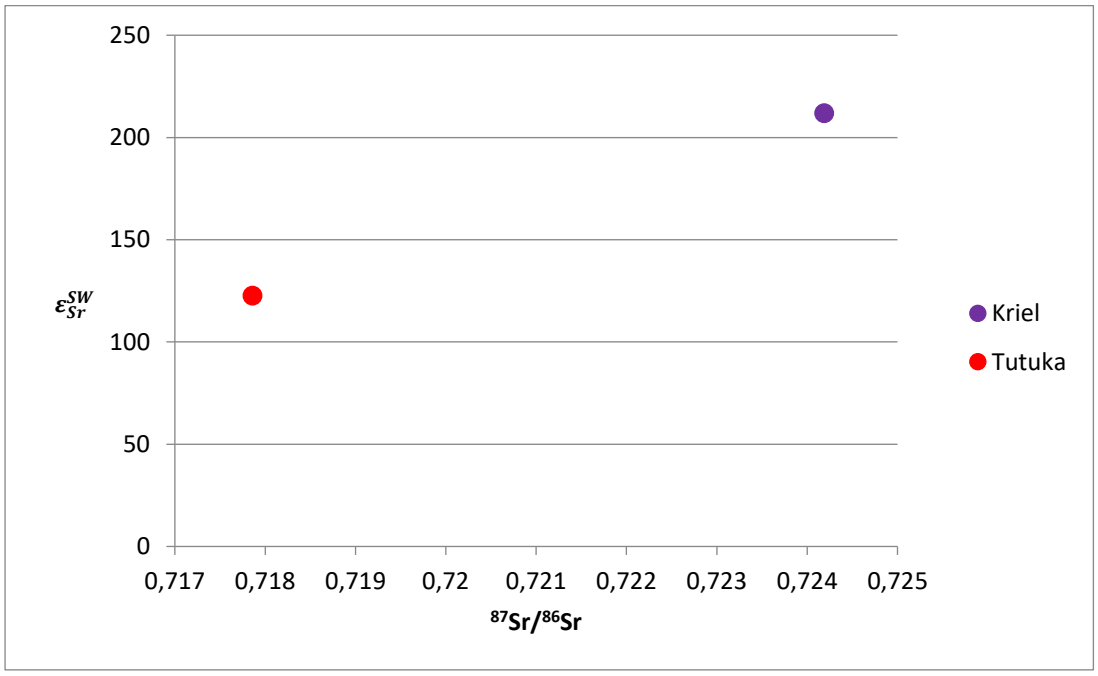


Figure 11: Variations in the strontium isotope composition of the CFA from the Tutuka and Kriel samples

The higher Sr isotopic composition of the Kriel sample also shows slightly higher trace metals and potentially toxic trace elements values compared to the Tutuka sample (Figure 12). The Kriel Power Station CFA has a higher abundance of Ba and Sr in comparison to the Tutuka Power Station however, the variation between Ba and Sr in the Tutuka Power Station CFA is less than that of the Kriel Power Station CFA.

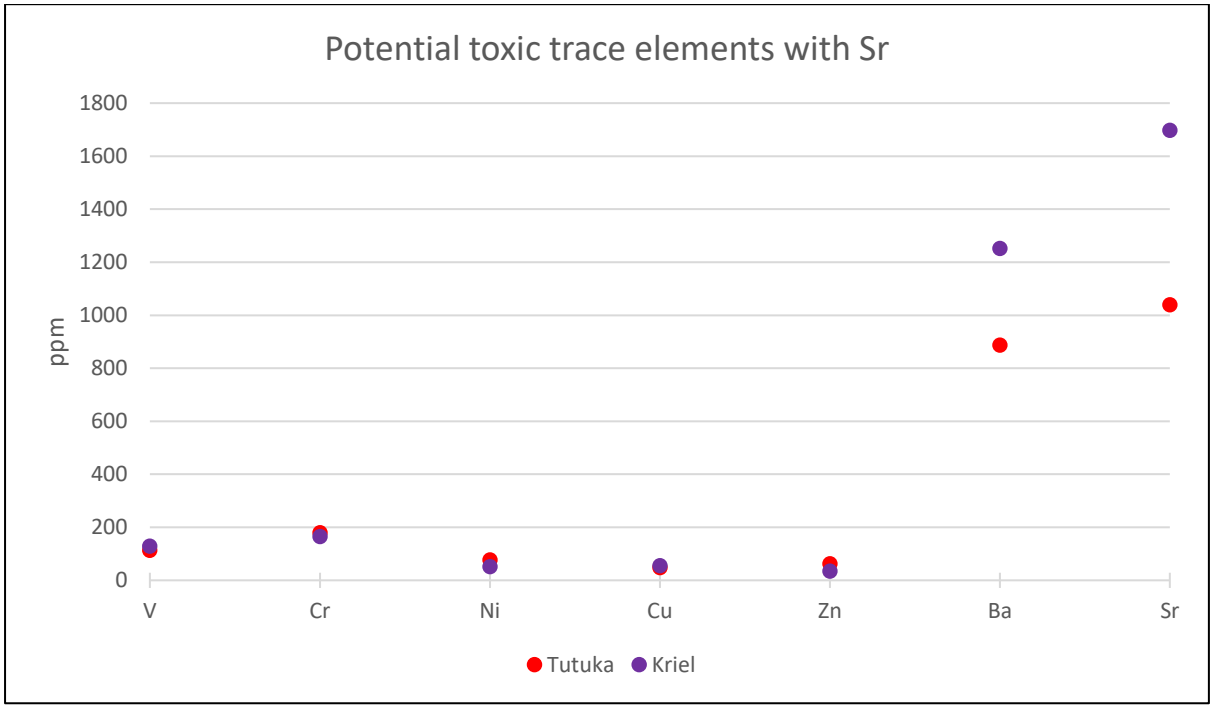


Figure 12: Potentially toxic trace elements plotted with Sr to show relationship between Sr and toxic trace element concentrations.

CHAPTER 5 - Discussion

5.1 Comparison of the mineral assemblages of the studied CFA samples

The results of PXRD analysis clearly show that the predominant mineralogical assemblages present in the CFA samples are silicates and Al-rich mineral phases. The dominant non-magnetic phases are represented by mullite and quartz, while the major magnetic minerals are hematite and magnetite. These results align with results obtained in the previous study by Alegbe et al. (2018) and Van der Merwe et al. (2014). A CFA sample from an undisclosed power station in the Mpumalanga Province, South Africa is characterised by the presence of hematite, magnetite, mullite, and quartz (Alegbe et al., 2018). The CFA samples from Eskom Lethabo Thermal Power Station have mullite and quartz as their main crystalline phases (Van der Merwe et al., 2014).

CFA samples consisted primarily of an amorphous glassy phase, with glassy cenospheres, ferrospheres, and quartz, which were derived from medium-rank C bituminous, inertinite-rich, high-ash coals (Wagner and Matiane, 2018). The presence of mullite and ettringite among the mineral assemblages of the studied CFA samples may be an indication that mineral transformation has occurred. The presence of mullite indicates the breakdown of kaolinite in the high-temperature coal combustion process (White and Case, 1990). Mullite is formed during the high-temperature comparative combustion of fine clay mineral particles (Dai et al., 2010). The presence of ettringite, a hydrated Ca-Al-sulphate hydroxide, in the Komati, Tutuka, and Kriel samples (Figures 6 and 7) suggests the interaction of water with Ca-bearing mineral phases (Kim and Hesbach, 2009) or from the chemical reaction between calcium aluminate and calcium sulphate (Akinyemi et al., 2020). The formation of ettringite requires the presence of a high pH (>11), excess water, sulphates, calcium, and aluminium sources (Hasset et al., 2005). The presence of ettringite in the Komati, Tutuka, and Kriel CFA samples indicates that, unlike for Grootvlei and Hendrina, the CFA was in contact with water exhibiting high pH values. Studies to investigate ettringite formation and the removal of oxy-anion species have been conducted and ettringite has theoretically demonstrated the potential for waste immobilisation (Chrysochoou and Dermatas, 2006). It is important to note that the formation of ettringite occurs after long-term exposure (Jones, 1995); therefore, the Grootvlei and Hendrina samples may be fresher and could explain the absence of ettringite. Ettringite is unstable in regards to

re-carbonation reactions, therefore it cannot be viewed as an ultimate sink for oxy-anions exposed to surface conditions (Jones, 1995).

From the presence of ettringite, it can also be deduced that the leaching and weathering process had already commenced in the CFA from Komati, Tutuka, and Kriel power stations. This leaching process appears not to be as pronounced in the CFA samples from Grootvlei and Hendrina power stations.

5.2 Potentially hazardous trace elements in CFA

Potentially hazardous elements, namely Ba, Cr, Cu, Ni, V, and Zn, were detected in the CFA samples (Table 6). From the trace elements considered to be hazardous, such as As, B, Cr, Cd, Hg, Pb, F, and Se (Kashiwakura et al., 2013), Cr is present in relatively high concentrations (Figure 13). The Cr concentrations in the South African samples range between 148.8 to 182.0 ppm and are much higher in comparison to the average concentrations of CFA from Australia at 69 ppm, Europe at 137 ppm, Canada, and the USA at 55 ppm (Riley, 2007). The concentrations of Cr in the CFA in this study are higher than the typical global value for Cr which is reported to be 100 ppm (Table 6; Ketris and Yudovich, 2009). The concentration of Cr in the studied samples is enriched in comparison to the typical global values (Figures 9 and 13).

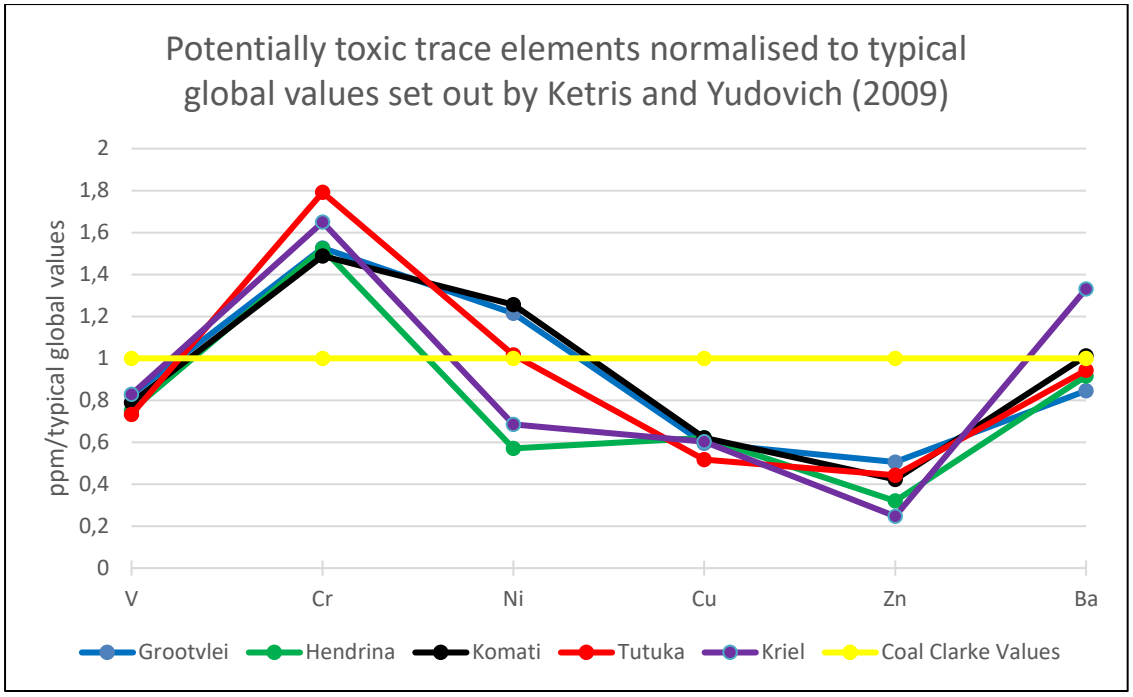


Figure 13: Potentially toxic trace elements detected in the studied CFA samples that were normalised to the typical global values set out by Ketris and Yudovich (2009)

There are two types of Cr usually present in CFA, the first one being Cr (III) which is considered insoluble and harmless, but can be harmful in high concentrations, and the second one being Cr (VI) which can be found in small amounts (4–9%, Sloss, 2007). The average concentration for Cr (VI) in CFA is 13 ppm, the majority of which reacts with Fe compounds within the CFA to produce Cr (III, Sloss, 2007). The high concentrations of Cr in the studied CFA could be cause for concern, largely due to the Cr likely being Cr (III) which is harmful in high concentrations (Sloss, 2007).

The high values of Cr in the studied CFA perhaps can be linked to the composition of the parental coal. Wagner et al. (2021) show a general enrichment of Cr in Permian coals in South Africa, linked to the large Cr quantities found in the Precambrian Bushveld Complex. Wagner et al. (2021) also reported a decrease in Cr concentrations with increasing distance of a coalfield from the Bushveld Complex (Wagner et al., 2021). This decrease in Cr contents with increased distance from the Bushveld Complex is not consistent with the results of this study. The sample from Komati shows the lowest Cr concentrations and the location of this power plant is closer to the Bushveld compared to the other power plants considered in this study.

Perhaps the concentrations of Cr in the analysed CFA samples in this study are not directly dependent on the original chemical compositions of the parental coal. At the moment, this cannot be tested, as the trace element compositions of the parental coal sample were not available for this research. Another cause of the variability of Cr concentrations among the samples may be linked to pH conditions. The solubility of oxy-anions such as Cr, V, Mo, As, and Se is favoured in high pH conditions, whereas the solubility of heavy metals such as Pb, Zn, Cu, and Ni is favoured in low pH conditions (Kim and Hesbach, 2009). Oxy-anions such as As, B, Cr, Mo, Se, and V are known to participate in the formation of ettringite (Hassett et al., 2005). This may suggest that the elemental concentrations of V and Cr in the studied CFA samples may have previously been higher than what is currently reported in Table 6, as their concentrations may have decreased due to the formation of ettringite.

Ni and Ba are two other potentially toxic trace elements that show enrichment above the normalised typical global value (Figure 13). The studied CFA showed higher concentrations of Ni than typical global values excluding the Hendrina and Kriel CFA samples, which had lower concentrations. Similarly, the CFA showed higher concentrations than the typical global values for Ba, excluding the Grootvlei and Tutuka CFA, which had lower concentrations of Ba. Ni, Cu, and Zn (below the normalised typical global values set out by Ketris and Yudovich, 2009), indicating that although these potentially toxic trace elements are present within the CFA, they are not present in potentially hazardous concentrations.

5.3 Classification of the CFA samples

ASTM International (2017) presents standard specifications in CFA that are important for cement manufacturing. Using the ASTM International (2017) standards used for classifying CFA in the cement manufacturing industry the investigated CFA samples can be classified according to the standards set out in Table 8.

Table 8: Chemical requirements for different classes of CFA (ASTM International, 2017)

	Class		
	N	**F**	**C**
$SiO_2 + Al_2O_3 + Fe_2O_3$, min. %	70.0	70.0	50.0
SO_3, max. %	4.0	5.0	5.0
Moisture content, max. %	3.0	3.0	3.0
LOI, max. %	10.0	6.0	6.0

Based on the major elements in this study (Table 5) and according to the ASTM International (2017) standards, the studied CFA samples, except for the sample from Komati Power Station, may be classified as Class F. The sample from Komati is characterised by much higher LOI values compared to the other samples (9.34%, Table 5). According to the classification in Table 8, the Komati CFA sample with LOI values greater than 6% belongs to Class N (Table 8).

The dominance of Class F CFA, as detected in this study, is consistent with previous studies by Van der Merwe et al. (2014) on CFA generated by the Lethabo Power Station, in the Free State Province of South Africa, as well as a previous study by Lieberman et al. (2018) on an unspecified South African power station. The Komati sample is not a unique example of Class N CFA in South Africa as the weathered CFA studied by Akinyemi et al. (2020) is also classified as Class N CFA.

Class F CFA, such as samples from Hendrina, Tutuka, Kriel, and Grootvlei Power Stations, are attributed to the burning of bituminous and some sub-bituminous coal (Kesharwani et al., 2017). Class N CFA, like the sample from the Komati Power Station, may be derived from the burning of natural pozzolans such as calcined volcanic ash, calcined shale, etc (Kesharwani et al., 2017). Class C CFA, which was not detected among the samples in this study, is derived from the burning of some sub-bituminous and lignite coals (Kesharwani et al., 2017). South African CFA is commonly classified as Class F CFA, making the classification of the Komati Power Station CFA as Class N CFA an anomaly. This may be attributed to chemical changes occurring on the Komati Power Station CFA possibly due to weathering and/or contamination.

Coal fly ash samples can also be classified using the system mentioned in Vassilev and Vassileva (2007), which is based on four chemical characteristics listed in Table 9.

Table 9: CFA classification criteria as discussed in Vassilev and Vassileva (2007)

Groups	Classification Type	Ratios
I	Silico-aluminate	$SiO_2/Al_2O_3 \geq 2$ and CaO < 15%
II	Alumino-silicate	$SiO_2/Al_2O_3 < 2$ and CaO < 15%
III	Limesulphate	CaO > 15% and $SO_3 > 3\%$
IV	Basic	CaO > 15% and $SO_3 < 3\%$

According to the CFA classification criteria of Vassilev and Vassileva (2007), the samples from Grootvlei, Hendrina, Tutuka, and Kriel once more are distinguishing themselves from the sample from Komati. Grootvlei, Hendrina, Tutuka, and Kriel CFA samples are classified as alumino-silicate type (Group II, Table 9), while the Komati CFA belongs to the silico-aluminate type CFA (Group I, Table 9). Unlike the Pan et al. (2018) study which found silica-aluminate to be the most dominant REY occurrence in the CFA, this study has a much higher occurrence of alumina-silicate type CFA.

The weathered and fresh CFA investigated in a previous study by Akinyemi et al. (2020) from an undisclosed power station in South Africa can be classified as silico-aluminate type CFA, similar to the Komati sample of this study. The CFA samples in the Akinyemi et al. (2020) study contain $SiO_2/Al_2O_3 = 2.01$ and CaO of 5.26% for the fresh CFA, and $SiO_2/Al_2O_3 = 2.23$, and a CaO of 5.08% for the weathered CFA. The Lethabo Thermal Power Station CFA studies by Van der Merwe et al. (2014) and the South African CFA analysed by Lieberman et al. (2018) can be classified as alumino-silicate type, having $SiO_2/Al_2O_3 = 1.45$ and CaO of 5.06%, and $SiO_2/Al_2O_3 = 1.32$ and CaO of 9.50%, respectively. Therefore, they can be classified as Group II similar to the CFA from the Grootvlei, Hendrina, Kriel, and Tutuka Power Station.

Akinyemi et al. (2020) focused on examining 20-year-old, unsaturated, and weathered drill core ash along with fresh CFA. The similarities in the classification of the CFA could be a result of the CFA being exposed to similar environmental conditions over a

prolonged period. There is a possibility that the Komati CFA examined in this study may have been exposed to weathering before being analysed, resulting in a shift in classification from Class F to Class N. The presence of ettringite in the mineralogy of the Komati CFA (Figure 6) could be indicative of the CFA having undergone weathering. The reported LOI for the Komati CFA is reported as 9.34, which is noticeably higher in comparison to the Grootvlei, Hendrina, Tutuka, and Kriel CFA samples, which have LOIs of 1.84, 3.87, 3.60, and 2.67, respectively.

5.4 Strontium isotopic compositions

The global mean value of Sr in CFA is 740 ppm (Ketris and Yudovich, 2009); however, values of up to ca. 3000 mg/kg can be reached (Hurst et al., 1991). All the investigated CFA samples in this study have Sr contents above the global mean value (Table 6). The Kriel sample shows the highest Sr value of 1759.0 ppm followed by Hendrina with a Sr value of 1548.7 ppm, Komati with a Sr value of 1040.7 mg/kg, Tutuka with a Sr value of 957.0 ppm, and lastly, the lowest Sr contents are in Grootvlei with a concentration of 810.3 ppm.

The lack of previous Sr isotope studies on CFA in South Africa does not allow a local comparison of the $^{87}Sr/^{86}Sr$ data of this study. Therefore, the Sr concentration and the $^{87}Sr/^{86}Sr$ results are here compared with the bulk CFA data from the three largest coal-producing basins in the United States of America (Figures 14 and 15, Wang et al., 2020).

The CFA samples in this study show lower Sr concentrations than samples from the Powder River Basin (PRB), and higher Sr contents than the CFA produced in the Illinois Basin (ILL) and Appalachian Basin (APP, Figure 14).

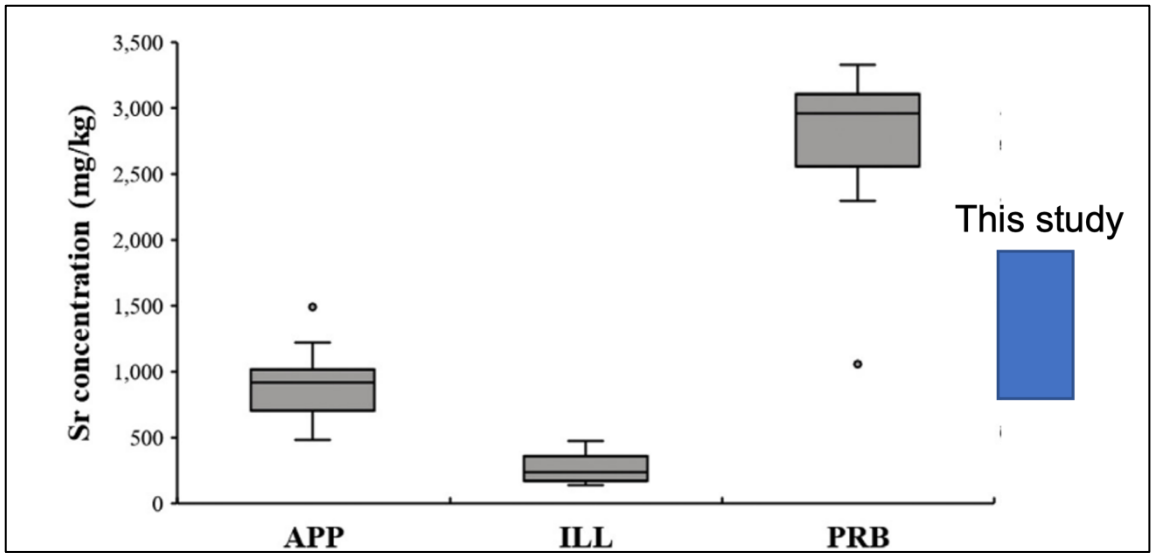


Figure 14: Strontium concentrations of bulk fly ash in this study are compared with data from different coal basins in the United States of America APP: Appalachian Basin, ILL: Illinois Basin and PRB: Powder River Basin (modified from Wang et al., 2020).

The variation in the Sr concentrations in the samples from coal-producing basins in the United States of America has been attributed to the differences in Sr-bearing minerals in the coal which was mined (Wang et al., 2020). However, the research fails to detail which Sr-bearing minerals are being referred to. It was not possible to determine which Sr-bearing minerals occurred in the CFA of this study. To do this, it is necessary to perform a leaching/extraction procedure on the samples as described in Brubaker et al. (2013) or to analyse the CFA using a TESCAN Integrated Mineral Analyser (TIMA) to gain mineralogical, textural, and chemical information on the parent coal and its CFA for comparison. Such analyses were not included as part of this study, but this could potentially be done for future studies.

The Sr isotopic composition of the CFA sample from Kriel is higher than the three largest coal-producing basins in the United States of America (Figure 15). The Sr isotopic composition of the CFA sample from Tutuka is higher than for two of the three major coal-producing basins in the United States of America (Appalachian and Powder River basins) and comparable to data from the Illinois Basin (Figure 15). Wang et al. (2020) attributed the difference in Sr isotope concentration to the difference in Sr-bearing minerals in the feed coal. Similarly, the Kriel and Tutuka feed coals may have more Sr-bearing minerals than those found in the feed coals of the Appalachian, Powder River, and Illinois basins.

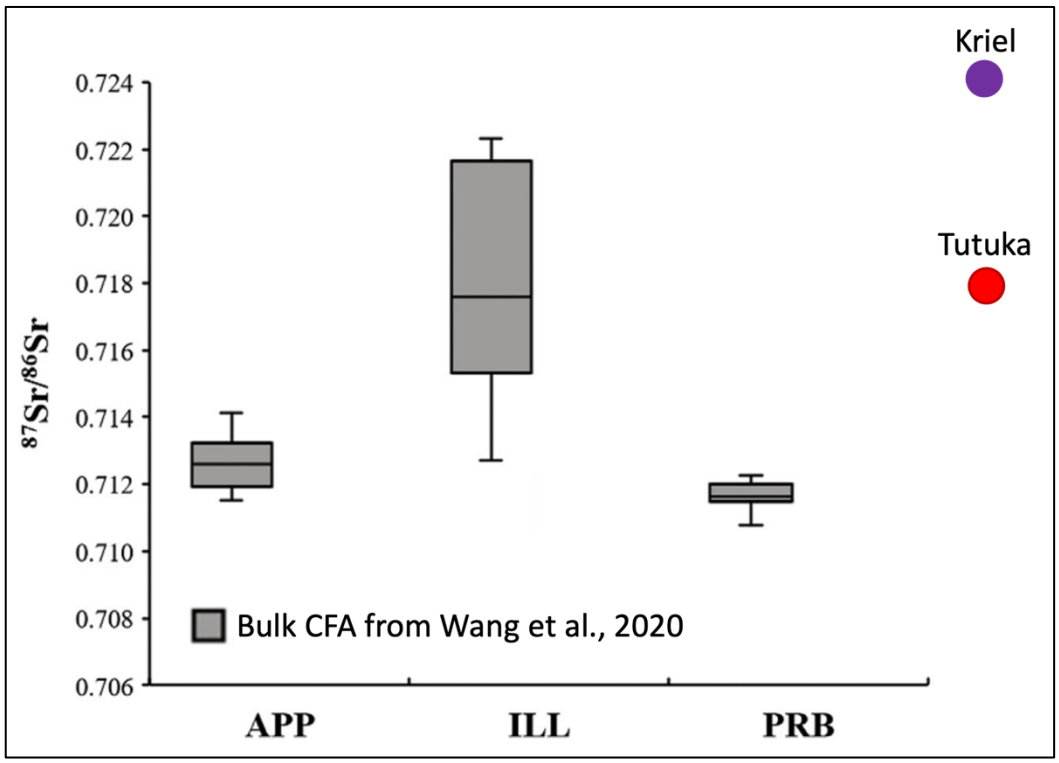


Figure 15: Comparison of the $^{87}Sr/^{86}Sr$ ratios of bulk ash fly ash samples sourced from different coal basins in the United States of America. APP: Appalachian Basin, ILL: Illinois Basin, and PRB: Powder River Basin and the data of this study from Tutuka and Kriel (modified from Wang et al., 2020).

To see whether a correlation exists between Sr and heavy metals, a statistical software called eViews 12 (a statistical package for Windows, www.eviews.com) was used to generate a correlation table (Table 11).

To test the relationship between Sr and heavy metals in the CFA samples a correlation test was performed and the results are displayed in Table 10. The correlation test shows that Sr has a strong positive correlation with Ba, and a slight positive correlation with Cr and V (Figure 16), suggesting that an increase in Sr within CFA will result in an increase in Ba, Cr, and V in CFA. The Sr also has a strong negative correlation with Co, Ni, Tl, and Zn and a very slight negative correlation with Pb, suggesting an increase in Sr within CFA will result in a decrease in Co, Ni, Tl, Zn, and Pb in CFA.

Table 10: Correlation between Sr and the heavy metals detected within the CFA samples

	BA	CO	CR	NI	PB	SR	TL	V	ZN
BA	1	-0.5730882...	0.70871887...	-0.1941057...	-0.0205641...	0.74945043...	-0.4155728...	0.44400294...	-0.5909077...
CO	-0.5730882...	1	-0.6850747...	0.82093010...	0.65165308...	-0.7184999...	0.87913994...	0.35906915...	0.76088776...
CR	0.70871887...	-0.6850747...	1	-0.5238207...	-0.6511724...	0.46643898...	-0.7596444...	-0.1542801...	-0.2995257...
NI	-0.1941057...	0.82093010...	-0.5238207...	1	0.69374286...	-0.6134100...	0.95167178...	0.46088221...	0.66378453...
PB	-0.0205641...	0.65165308...	-0.6511724...	0.69374286...	1	-0.0295883...	0.75470489...	0.84373307...	0.05974770...
SR	0.74945043...	-0.7184999...	0.46643898...	-0.6134100...	-0.0295883...	1	-0.6495988...	0.33805599...	-0.9554850...
TL	-0.4155728...	0.87913994...	-0.7596444...	0.95167178...	0.75470489...	-0.6495988...	1	0.39562050...	0.62810044...
V	0.44400294...	0.35906915...	-0.1542801...	0.46088221...	0.84373307...	0.33805599...	0.39562050...	1	-0.1808477...
ZN	-0.5909077...	0.76088776...	-0.2995257...	0.66378453...	0.05974770...	-0.9554850...	0.62810044...	-0.1808477...	1

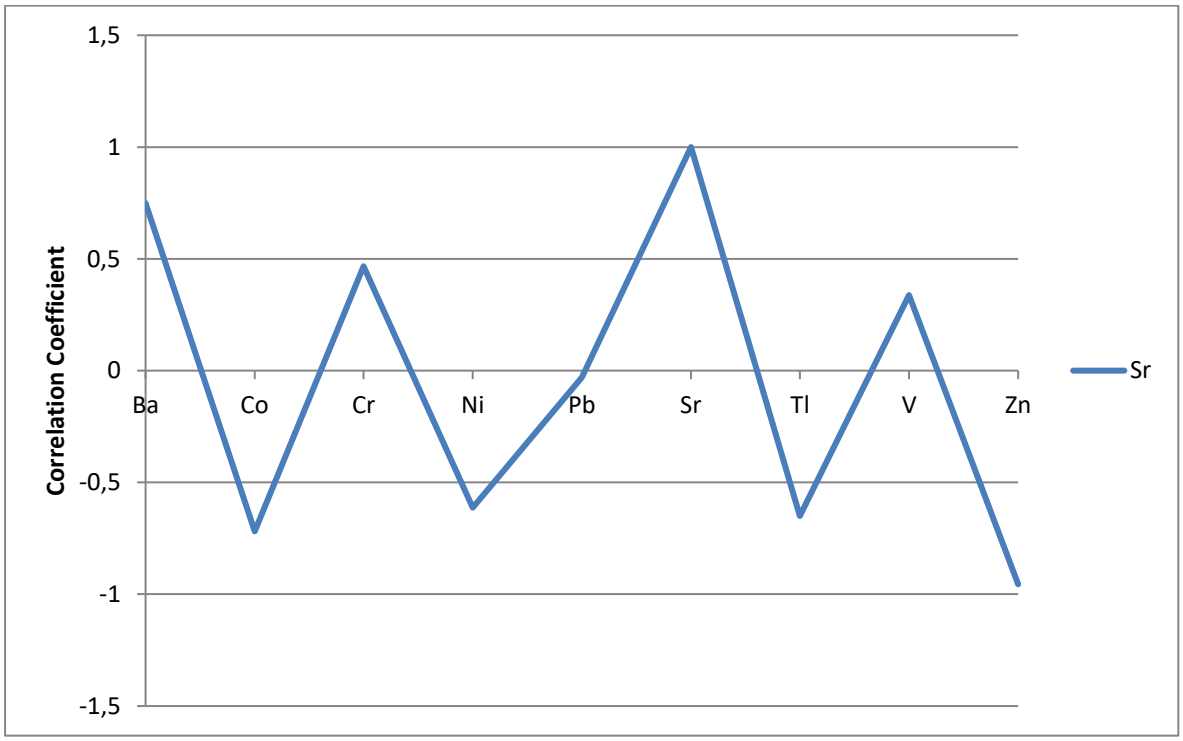


Figure 16: Correlation between Sr and the potentially toxic trace elements within the CFA samples

Due to the CFA samples in this study having a Sr concentration that is higher than the global mean value of ca. 740 ppm (Ketris and Yudovich, 2009), the CFA may have the potential of being hazardous to the environment. A leaching procedure would need to be conducted to fully understand the correlation between Sr and the mobility of toxic trace elements. Spivak-Birndorf et al. (2012) concluded that certain strongly bound elements of environmental concern could be released into the environment due to the changing Sr isotope ratio in the waters interacting with coal utilisation products such as CFA. More studies and reliable tests would need to be done to investigate the extent to which CFA retains and release toxic trace elements into the environment

under various pH and redox conditions (Hassett et al., 2005). This will allow for better, more appropriate long-term storage solutions to be established for CFA.

5.5 CFA as a potential source of REE

The increase in global demand to transition to green clean energy is putting a lot of stress on the coal and 'coal burning' industry. However, the shift to alternative green ways of energy production will happen progressively, and there is a high likelihood that coal will still be used for energy production in South Africa in the foreseeable future, due to the low cost of coal energy and the abundance of coal resources (Seredin et al., 2013). Since the burning of feed coal results in the production of large quantities of CFA, novel applications for the recycling of CFA may assist in transforming a potentially hazardous by-product of coal-fired power generation into a potential new revenue stream and improvements in the coal industry value chain in South Africa. Recent research shows that the trace element concentrations of CFA are playing a role in the transformation of the industrial ecology and circular economy. There are already novel applications for recycled CFA, where CFA is itself becoming a commodity for the production of alumina (Matjie et al., 2005), oxygen in reduction reaction (Fernandes et al., 2021), and REY (Seredin and Dai, 2012; Seredin et al., 2013; Wagner and Matiane, 2018).

The development of new forms of clean energy, such as hybrid electric vehicles (HEV) and a high-efficiency lighting, requires high supply and extraction of critical raw metals, such as REE, Y, and Sc. Similar to the research by Wagner and Matiane (2018), this study investigated the concentration of rare earth elements (REE), including yttrium (REY) along with scandium (Sc), to determine whether the CFA could be a potential source for REY + Sc (Table 11 and Figure 17).

The CFA samples in this study together with CFA samples analysed by Wagner and Matiane (2018) have abundances that are well above the average upper continental crustal abundance values (Table 11 and Figure 17). Furthermore, the CFA from South African power stations is more enriched in REY + Sc compared to CFA from Jungar Power Station in China, for example (Dai et al., 2010, Figure 17).

Table 11: Comparison of the REY + Sc between the upper continental crust (UCC) values from Taylor and McLennan (1985) and the CFA samples from the South African coal-fired power stations.

REY +Sc	REY Concentration (ppm)					
	Upper Continental Crust (UCC)[a]	Grootvlei Power Station, SA	Hendrina Power Station, SA	Komati Power Station, SA	Tutuka Power Station, SA	Kriel Power Station, SA
La	30.0	97.2	132.3	102.9	89.7	109.1
Ce	64.0	202.9	265.4	212.8	181.8	223.9
Pr	7.1	21.1	26.7	21.8	19.5	22.8
Nd	26.0	77.3	95.3	78.5	72.2	84.8
Sm	4.5	14.5	17.4	14.7	13.5	15.4
Eu	0.88	2.8	3.1	2.7	2.6	2.8
Gd	3.8	13.4	15.7	13.6	12.6	13.9
Tb	0.8	1.9	2.3	2.0	1.8	2.1
Dy	3.5	12.1	13.9	11.8	11.1	12.3
Ho	0.8	2.4	2.6	2.3	2.3	2.4
Er	2.3	6.7	7.2	6.3	6.1	6.5
Tm	0.33	1.0	1.1	0.9	0.9	0.9
Yb	2.2	6.4	6.8	5.9	5.8	6.0
Lu	0.32	0.9	0.9	0.8	0.8	0.8
Y	22.0	67.1	70.4	62.1	60.6	61.8
Sc	11.0	29.6	27.8	28.1	24.3	26.0

[a] Taylor and McLennan (1985)

There appears to be a general similarity in the overall distribution of REY + Sc for the five power stations. The Hendrina Power Station shows variability in its concentrations of La, Ce, and Nd, which are higher than the concentrations of the other four power stations. The lowest concentrations of Ce can be found in the Tutuka Power Station CFA - although the Tutuka Power Station CFA does show a trend of having lower concentrations of REY + Sc in comparison to the other four CFA samples – there appears to be a much larger variation in the difference in Ce concentration.

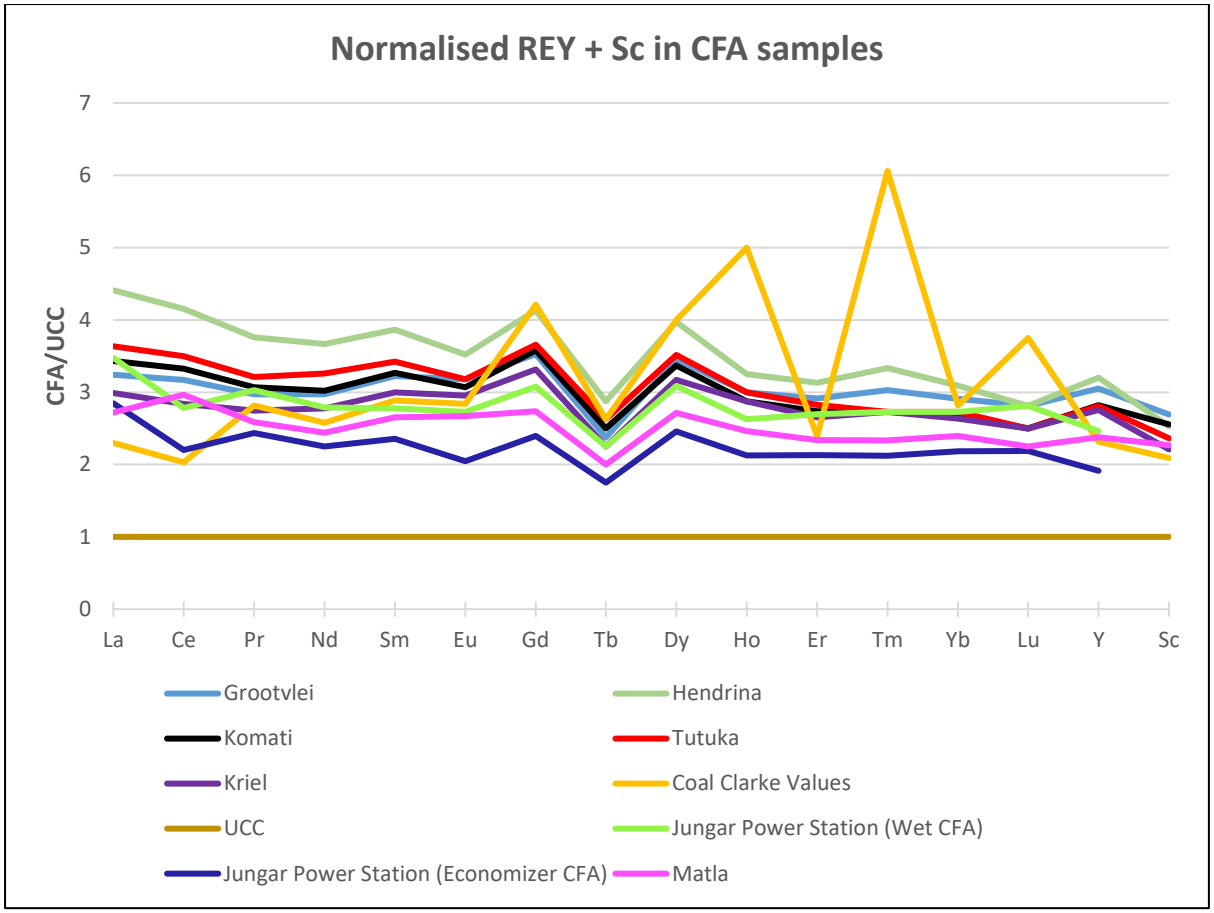


Figure 17: The normalised UCC REY + Sc values of the Grootvlei, Hendrina and Komati sample along with the normalised UCC REY + Sc (incl. Jungar Power Station sourced from Dai et al., 2010) of the CFA samples sourced from the Wagner and Matiane (2018) study (UCC data from Taylor and McLennan, 1985)

According to the Seredin and Dai (2012) classification (Figure 18), the potential sources of REY are classified into three economic clusters, namely: cluster I, which is indicative of an unpromising source, cluster II, indicative of a promising source and finally, cluster III indicating a highly promising source. In order to evaluate the high REY ash in terms of potential industrial value, a $REY_{def,\ rel}$% vs C_{outl} graph was plotted by Seredin and Dai (2012) as shown in Figure 18. The $REY_{def,\ rel}$% is described as the percentage of critical elements in the total REY (Seredin and Dai, 2012).

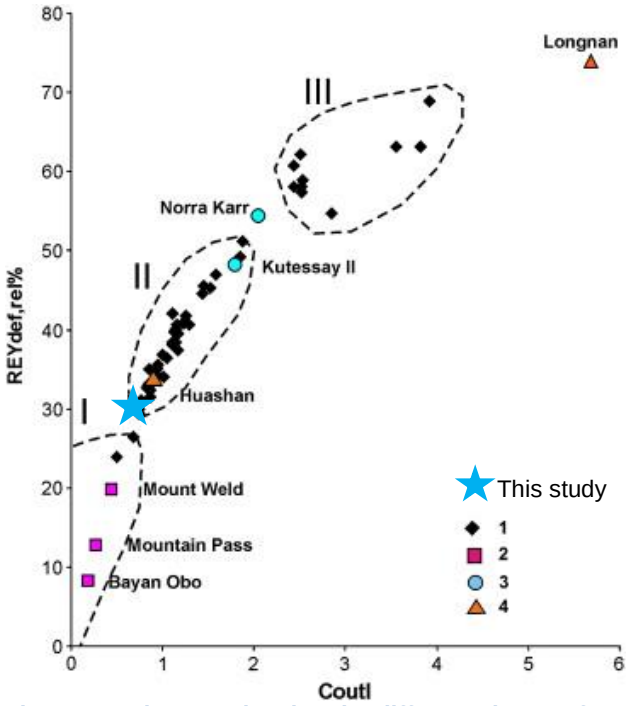


Figure 18: Diagram showing the different clusters for potential REY sources: I. unpromising sources; II. promising sources; and III. highly promising sources with 1 – REE-rich coal ashes; 2 – carbonatite deposits; 3 – hydrothermal deposits and; 4 – weathered crust elution-deposited (ion-absorbed) deposits and the blue star being the CFA in this study (Modified from Seredin and Dai, 2012)

The C_{outl} formula is as follows:

C_{outl} = (Nd + Eu + Tb + Dy + Er + Y/∑REY)/(Ce + Ho + Tm + Yb + Lu/∑REY)

The Grootvlei, Hendrina, Komati, Tutuka, and Kriel have C_{outl} values of 0.787, 0.693, 0.734, 0.728, and 0.806 and $REY_{def,rel}$% values of 31,83%, 29.06%, 30.33%, 27.69%, and 30.08%, placing the samples into category II (Figure 18, blue star) and they can therefore be classified as promising sources for REY extraction. The study into the potential for REY extraction in CFA was updated by Dai et al. (2017) which consists of plotting REY oxides vs $REY_{def,rel}$% with the requirement that REY oxide content is higher than 1000 ppm. Taking that into account, the Grootvlei, Hendrina, Komati, Tutuka, and Kriel samples do not qualify as potential sources for REY extraction due to the samples not having a REY oxide content that is higher than 1000 ppm.

A graph was produced to compare the normalised REY values of the CFA in this study with four major REE ore deposits located in Southern Africa, namely the Lofdal, Glenover (in-situ ore), Zandkopsdrift and Steenkampskraal deposits as discussed in Harmer and Nex (2016, Figure 19).

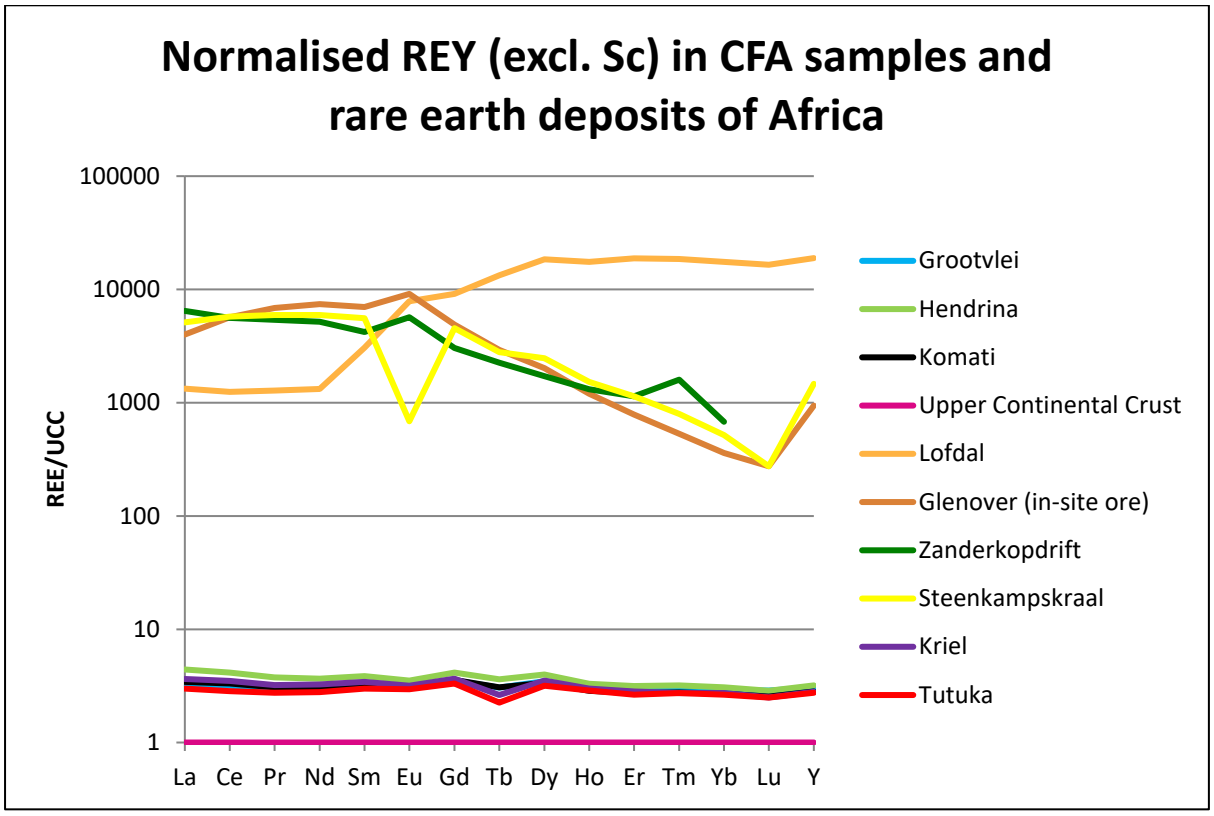


Figure 19: Comparison of the normalised UCC REY values of the Grootvlei, Hendrina and Komati CFA samples with values of the REE ore deposits sourced from the Harmer and Nex (2016) (UCC data from Taylor and McLennan, 1985)

The comparison clearly shows that the Grootvlei, Hendrina, Komati, Tutuka, and Kriel CFA samples have a very low abundance of REY in comparison to the REE ore deposits, which have REE concentrations in the order of % and not ppm and enrichments well above the average upper continental crustal (Figure 19). At the same time, a distinct difference in the resource tonnage of the REE ore deposits and the CFA stockpiles is known. The rare earth deposits have tonnages of 2.88 Mt for the Lofdal deposit, 7.41 Mt for the Glenover (in-situ ore) deposit, 22.7 Mt for the Zanderkopsdrift deposit, and 0.474 Mt for the Steenkampskraal deposit (Harmer and Nex, 2016). CFA in South Africa is produced daily in very high quantities, reaching up to >25Mt of CFA being produced annually by coal-fired power stations (Ash Management in Eskom, 2021). Although the REY enrichment of the CFA samples is low in comparison to the REE ore deposits, the quantity of CFA is much larger than most REE ore deposits. The CFA stockpiles can be considered as potential low-grade disseminated REY mineralisations. The possibility of exploiting these low-grade REY

resources can only be tested by metallurgical studies, such as Mokoena et al. (2022) have shown.

CHAPTER 6

6.1 Conclusion

The mineralogical and geochemical characterisation of CFA in South African coal-fired power stations has become increasingly important over the years as more and more coal is burned in power stations to generate electricity. High quantities of CUP and CFA are accumulated daily in stockpiles, where they are exposed to rainwater, wind, erosion, and weathering. This exposure can result in the leaching of potentially toxic trace elements into the environment which can become potentially hazardous. Therefore, a detailed study on the mineralogy and trace elements geochemistry may help in better understanding the availability of potentially toxic trace elements to leaching and weathering and in finding alternative uses for CFA as well as better storage solutions.

In this study, we assessed and compared the mineralogy, major and trace elements, and radiogenic Sr isotopic compositions of five CFA samples from distinct power plant stations in Mpumalanga, South Africa, namely Komati, Tutuka, Grootvlei, Hendrina, and Kriel Power Stations. The XRD analysis revealed the predominant composition present in the CFA samples as silicates and Al-rich phases, with quartz, mullite, hematite, and magnetite being detected in all the samples. The mineralogy in this study was found to be similar to the mineralogy described in South African power stations examined by Alegbe et al. (2018), Van der Merwe et al. (2014), and Fatoba (2008). Ettringite detected in the Komati, Tutuka, and Kriel samples is consistent with the findings of Akinyemi et al. (2020) The presence of ettringite may be indicative of a phase change occurring within the samples as a result of water interacting with the CFA under high pH conditions (Hasset et al., 2005). This could also be indicative of the CFA previously being exposed to environmental conditions that resulted in weathering.

High Cr concentrations were detected in the CFA analysed in this study, which ranked them as being above the averages reported for CFA in Australia, Europe, Canada,

and the United States of America (Riley, 2007). This high Cr concentration may represent a possible cause for environmental concern. In comparison to the typical global values for coal fly ash, as determined by Ketris and Yudovich (2009), the CFA samples in this study show a general similarity in trace element concentration distribution. The studied CFA samples show a much higher concentration of Ti and Sr in comparison to typical global values and very low concentrations of Cu and Zn.

The Sr isotopic analysis revealed that the studied CFA samples from this study have Sr concentrations above the global mean values, warranting further study into the leaching behaviour of Sr and the correlation between the leaching of Sr and trace elements. The lack of available Sr isotopic data for South African CFA did not allow comparison with CFA samples from other power stations in South Africa. Therefore, the $^{87}Sr/^{86}Sr$ ratios data from this study have been compared with data from similar studies conducted in the United States of America. The comparison shows that the $^{87}Sr/^{86}Sr$ ratios of the Kriel CFA are higher than the three largest coal-producing basins in the United States of America, namely the Appalachian Basin, the Illinois Basin and the Powder River Basin. The $^{87}Sr/^{86}Sr$ ratio of the Tutuka CFA was found to be higher than the Appalachian Basin CFA, and The Powder River Basin CFA and comparable to data from the Illinois Basin CFA. This can be attributed to the higher quantity of Sr-bearing minerals in the feed coals mined at the Kriel and Tutuka power stations.

The studied samples were examined to determine the likelihood of them being potential sources for REY + Sc. To determine whether the CFA samples could be potential sources for REY + Sc, the samples were normalised to the upper continental crust values. The REY + Sc values of the investigated CFA samples all fall above the Earth's upper continental crust values set out by Taylor and McLennan (1985). Significantly high values of La, Ce, Pr, Nd, and Y were observed in the Grootvlei, Hendrina, Komati, Tutuka, and Kriel samples in comparison to the upper continental crust values, and they ranked higher than the average global values for the same elements in CFA. Upon plotting the $REY_{def,\ rel}$% vs C_{outl} of the Grootvlei, Hendrina, Komati, Tutuka, and Kriel samples, it was concluded that the samples could be promising sources for REY extraction. However, in light of updated studies into the potential sources for REY extraction (Dai et al., 2017), the Grootvlei, Hendrina, Komati, Tutuka, and Kriel CFA samples do not meet the set criteria and are therefore not

considered potential sources for REY extraction. The comparison of the REY concentrations of the Grootvlei, Hendrina, Komati, Tutuka, and Kriel CFA samples and natural samples from well-known REY ore deposits clearly shows that REE ore deposits have a significantly higher enrichment in REY. However, CFA is generated at large quantities of >25Mt annually in South Africa which is significantly larger than most REE ore deposits. Therefore, the CFA stockpiles can be considered as potential low-grade disseminated REY mineralisation. The possibility of exploiting these low-grade REY resources and productive metallurgical extraction of the REY from the mineral phases is, however, still challenging, as the study of Mokoena et al. (2020) has shown.

6.2 Limitations

A few research limitations have been encountered during the course of this project. Firstly, the inability to gain access to CFA, despite numerous attempts at contacting Eskom officials. The CFA samples analysed in this study could be accessed only in August 2021 and only five samples could be secured for this study, thanks to the donation and support of colleagues from the School of Metallurgical Engineering of Wits University and the Department of Geology of the University of Johannesburg.

Another limitation is related to limited access to lab facilities and offices due to COVID restrictions during the entire course of 2021. This limitation considerably hindered the progress of the research from the very beginning.

Lastly, the possibility to conduct Sr isotope analysis only on two of the five CFA samples. This limitation is due to the closure of the Wits Isotope Geoscience Laboratory (WIGL) at The University of the Witwatersrand for renovation purposes in September 2021. Since samples were only obtained in August (2021), there was insufficient time to process all the samples, and the WIGL is the only facility in South Africa where the method of chemical separation of Sr isotopes is set up. The WIGL facility is still closed now, in October 2022, after 1 year. This was not envisaged one year ago and therefore, I also had no chance to complete this part of the analytical work as part of the final revision of the thesis. The time constraints resulting from the closure of the lab influenced the study, as a more thorough analysis could not be

conducted, leading to the inability to fully answer one of the research questions. Data generated by this study will, however, be relevant in future studies.

6.3 Recommendations

Future recommendations for the study into the geochemistry and Sr isotope characteristics of CFA generated in South African coal-fired power stations include:

1) obtaining a variety of CFA samples from various coal-fired power stations in South Africa to do a thorough comparative study,
2) conducting leaching experiments on the CFA to understand the solubility and bioavailability of the trace elements in CFA under various environmental conditions,
3) comparing the water-soluble fractions of Sr within the South African CFA to note the differences between the bulk and water-soluble Sr isotopic compositions in CFA and
4) conducting a study into the REY + Sc contents of South African CFA and whether such CFA qualifies as potential sources for REY extraction.

In order to fully understand the solubility and bioavailability of the trace elements as well as the critical parameters of ettringite formation under various conditions, it is recommended that a leaching experiment be conducted. Lastly, a detailed in-situ mineralogical-elemental mapping should be undertaken to better understand the relationship and distribution of metals and each mineral phase within representative CFA samples. This can be undertaken using the TIMA equipment, in the School of Geosciences, University of the Witwatersrand, and TIMA mapping will help in the elemental and mineralogical distribution of various CFA samples which could, in turn, inform any future metallurgical investigations for extraction of critical metals, such as REY from CFA.

References

Akinyemi, S.A., Gitari, W.M., Akinlua, A. and Petrik, L.F., 2012. Mineralogy and geochemistry of sub-bituminous coal and its combustion products from Mpumalanga Province, South Africa. *Analytical chemistry*, pp.47-70.

Akinyemi, S.A., Gitari, W.M., Thobakgale, R., Petrik, L.F., Nyakuma, B.B., Hower, J.C., Ward, C.R., Oliveira, M.L.S. and Silva, L.F.O., 2020. Geochemical fractionation of hazardous elements in fresh and drilled weathered South African coal fly ashes. *Environmental geochemistry and health*, *42*(9), pp.2771-2788.

Alegbe, J., Ayanda, O.S., Ndungu, P., Alexander, N., Fatoba, O.O. and Petrik, L.F., 2018. Chemical, Mineralogical and Morphological Investigation of Coal Fly Ash Obtained from Mpumalanga Province, South Africa, Res. *J. Environ. Sci*, *12*, pp.98-105.

An, D.L., 2014. *Critical Rare Earths, National Security, and US-China Interactions: A portfolio approach to dysprosium policy design*. The Pardee RAND Graduate School.

Ash Management in Eskom. 2021. *Fact Sheet: Ash Management in Eskom* [online] Available at: https://www.eskom.co.za/wp-content/uploads/2021/08/CO-0004-Ash-Management-Rev-15.pdf [Accessed 23 Mar. 2022].

ASTM International, 2017. *Standard Specification for Coal Fly Ash and Raw or Calcined Natural Pozzolan for Use in Concrete*. [online] Available at: https://www.astm.org/c0618-12.html [Accessed 10 Jan. 2022].

Ayanda, O.S., Fatoki, O.S., Adekola, F.A. and Ximba, B.J., 2012. Characterization of fly ash generated from Matla power station in Mpumalanga, South Africa. *E-Journal of Chemistry*, *9*(4), pp.1788-1795.

Bell, F.G., Bullock, S.E.T., Hälbich, T.F.J. and Lindsay, P., 2001. Environmental impacts associated with an abandoned mine in the Witbank Coalfield, South Africa. *International journal of coal geology*, *45*(2-3), pp.195-216.

Brubaker, T.M., Stewart, B.W., Capo, R.C., Schroeder, K.T., Chapman, E.C., Spivak-Birndorf, L.J., Vesper, D.J., Cardone, C.R. and Rohar, P.C., 2013. Coal fly ash interaction with environmental fluids: Geochemical and strontium isotope results from combined column and batch leaching experiments. *Applied Geochemistry*, *32*, pp.184-194.

Capo, R.C., Stewart, B.W. and Chadwick, O.A., 1998. Strontium isotopes as tracers of ecosystem processes: theory and methods. *Geoderma*, *82*(1-3), pp.197-225.

Chou, C.L., 2012a. Sulfur in coals: a review of geochemistry and origins. *International journal of coal geology*, *100*, pp.1-13.

Chou, M.I.M., 2012b. Fly Ash. In *Encyclopedia of Sustainability Science and Technology* (pp. 3820-3843). Springer New York.

Chrysochoou, M. and Dermatas, D., 2006. Evaluation of ettringite and hydrocalumite formation for heavy metal immobilization: Literature review and experimental study. *Journal of hazardous materials*, *136*(1), pp.20-33.

Dai, S., Zhao, L., Peng, S., Chou, C.L., Wang, X., Zhang, Y., Li, D. and Sun, Y., 2010. Abundances and distribution of minerals and elements in high-alumina coal fly ash from the Jungar Power Plant, Inner Mongolia, China. *International Journal of Coal Geology*, *81*(4), pp.320-332.

Dai, S., Xie, P., Jia, S., Ward, C.R., Hower, J.C., Yan, X. and French, D., 2017. Enrichment of U-Re-V-Cr-Se and rare earth elements in the Late Permian coals of the Moxinpo Coalfield, Chongqing, China: Genetic implications from geochemical and mineralogical data. *Ore Geology Reviews*, *80*, pp.1-17.

Department of Mineral Resources and Energy, 2015. *Energy Sources: Coal*. [online] Available at http://www.energy.gov.za/files/coal_frame.html [Accessed 14 Mar. 2021]

Eskom, 2016. *Eskom and ash management*. [online] Available at: https://www.eskom.co.za/news/Pages/Feb20.aspx [Accessed 14 Mar. 2021].

Faure G. 1977 Principles of isotope geology. New York, NY: John Wiley and Sons, Inc.

Faure, G. and Mensing, T.M., 2005. *Principles and applications*. John Wiley and Sons, Inc. pp. 897.

Fatoba, O.O., 2008. *Chemical compositions and leaching behaviour of some South African fly ashe.* (Masters dissertation, University of the Western Cape)

Fatoba, O. and Petrik, L., 2015. Stability of brine components in co-disposed fly ash-brine solid residue. In *World of coal ash (WOCA) conference, WOCA, Nashville, Tennasee TN, USA*.

Fernandes, D.M., Abdelkader-Fernández, V.K., Badenhorst, C., Bialecka, B., Guedes, A., Predeanu, G., Santos, A.C., Valentim, B., Wagner, N. and Freire, C.,

2021. Coal chars recovered from fly ash as promising electrocatalysts for oxygen reduction reaction. *International Journal of Hydrogen Energy*, *46*(70), pp.34679-34688.

GeoReM - Database on geochemical, environmental and biological reference materials (gwdg.de) [Accessed Sept. 2022].

Gitari, W.M., 2006. *Evaluation of the leachate chemistry and contaminants attenuation in Acid Mine Drainage by Fly Ash and its derivatives* (Doctoral dissertation, University of the Western Cape).

Gitari, W.M., Fatoba, O.O., Petrik, L.F. and Vadapalli, V.R., 2009. Leaching characteristics of selected South African fly ashes: Effect of pH on the release of major and trace species. *Journal of Environmental Science and Health Part A*, *44*(2), pp.206-220.

Gopinathan, P., Santosh, M.S., Dileepkumar, V.G., Subramani, T., Reddy, R., Masto, R.E. and Maity, S., 2022. Geochemical, mineralogical and toxicological characteristics of coal fly ash and its environmental impacts. *Chemosphere*, p.135710.

Hancox, P.J. and Götz, A.E., 2014. South Africa's coalfields—A 2014 perspective. *International Journal of Coal Geology*, *132*, pp.170-254.

Harmer, R.E. and Nex, P.A.M., 2016. Rare earth deposits of Africa. *Episodes*, *39*(2), pp.381-406.

Hassett, D.J., Pflughoeft-Hassett, D.F. and Heebink, L.V., 2005. Leaching of CCBs: observations from over 25 years of research. *Fuel*, *84*(11), pp.1378-1383.

Humphries, M., 2010. Rare earth elements: the global supply chain. Diane Publishing.

Hurst, R.W., Davis, T.E. and Elseewi, A.A., 1991. Strontium isotopes as tracers of coal combustion residue in the environment. *Engineering Geology*, *30*(1), pp.59-77.

Jones, D.R., 1995. The leaching of major and trace elements from coal ash. In *Environmental aspects of trace elements in coal* (pp. 221-262). Springer, Dordrecht.

Kashiwakura, S., Kumagai, Y., Kubo, H. and Wagatsuma, K., 2013. Dissolution of rare earth elements from coal fly ash particles in a dilute H2SO4 solvent. *Open Journal of Physical Chemistry, 3,* pp. 69-75.

Kesharwani, K.C., Biswas, A.K., Chaurasiya, A. and Rabbani, A., 2017. Experimental study on use of fly ash in concrete. *Int. Res. J. Eng. Technol*, *4*(9), pp.1527-1530.

Ketris, M.Á. and Yudovich, Y.E., 2009. Estimations of Clarkes for Carbonaceous biolithes: World averages for trace element contents in black shales and coals. *International journal of coal geology*, *78*(2), pp.135-148.

Khumalo, K.B., Ashwal, L.D., Hayes, B., Iaccheri, L.M., 2022. Evidence from Sr-Nd-Hf isotope evidence of a sublithospheric mantle source for the Neoarchean Westonaria komatiites. *In preparation*

Kim, A.G. and Hesbach, P., 2009. Comparison of fly ash leaching methods. *Fuel*, *88*(5), pp.926-937.

Kruse, K., Jasso, A., Folliard, K., Ferron, R., Juenger, M. and Drimalas, T., 2013. Characterizing fly ash. CTR Technical Report. *Centre for Transportation Research, The University of Texas, Austin*, pp.172

Izquierdo, M. and Querol, X., 2012. Leaching behaviour of elements from coal combustion fly ash: an overview. *International Journal of Coal Geology*, *94*, pp.54-66.

Lieberman, R.N., Knop, Y., Querol, X., Moreno, N., Muñoz-Quirós, C., Mastai, Y., Anker, Y. and Cohen, H., 2018. Environmental impact and potential use of coal fly ash and sub-economical quarry fine aggregates in concrete. *Journal of hazardous materials*, *344*, pp.1043-1056.

Matjie, R.H., Bunt, J.R. and Van Heerden, J.H.P., 2005. Extraction of alumina from coal fly ash generated from a selected low rank bituminous South African coal. *Minerals Engineering*, *18*(3), pp.299-310.

Mattigod, S.V., Rai, D. and Fruchter, J.S., 1990. Strontium isotopic characterization of soils and coal ashes. *Applied geochemistry*, *5*(3), pp.361-365.

Mishra, S.B., Langwenya, S.P., Mamba, B.B. and Balakrishnan, M., 2010. Study on surface morphology and physicochemical properties of raw and activated South African coal and coal fly ash. *Physics and Chemistry of the Earth, Parts A/B/C*, *35*(13-14), pp.811-814.

Mbugua, J.M., 2012. *Hydrogeochemical modeling of the speciation and leaching of fly ash co-disposed with water, brines and organics: a case study of Sasol-Eskom coal ash disposal, South Africa* (Doctoral dissertation, University of KwaZulu-Natal).

Mokoena, K., Mokhahlane, L.S. and Clarke, S., 2022. Effects of acid concentration on the recovery of rare earth elements from coal fly ash. *International Journal of Coal Geology*, p.104037.

Musyoka, N.M., 2009. *Hydrothermal synthesis and optimisation of zeolite Na-P1 from South African coal fly ash* (Doctoral dissertation, University of the Western Cape).

Norrish, K. and Hutton, J.T., 1969. An accurate X-ray spectrographic method for the analysis of a wide range of geological samples. *Geochimica et cosmochimica acta*, *33*(4), pp.431-453.

Nyale, S.M., Eze, C.P., Akinyeye, R.O., Gitari, W.M., Akinyemi, S.A., Fatoba, O.O. and Petrik, L.F., 2014. The leaching behaviour and geochemical fractionation of trace elements in hydraulically disposed weathered coal fly ash. *Journal of Environmental Science and Health, Part A*, *49*(2), pp.233-242.

Pan, J., Zhou, C., Liu, C., Tang, M., Cao, S., Hu, T., Ji, W., Luo, Y., Wen, M. and Zhang, N., 2018. Modes of occurrence of rare earth elements in coal fly ash: A case study. *Energy & Fuels*, *32*(9), pp.9738-9743.

Querol, X., Fernández-Turiel, J. and López-Soler, A., 1995. Trace elements in coal and their behaviour during combustion in a large power station. *Fuel*, *74*(3), pp.331-343.

Raja, R., Nayak, A.K., Shukla, A.K., Rao, K.S., Gautam, P., Lal, B., Tripathi, R., Shahid, M., Panda, B.B., Kumar, A. and Bhattacharyya, P., 2015. Impairment of soil health due to fly ash-fugitive dust deposition from coal-fired thermal power plants. *Environmental monitoring and assessment*, *187*(11), pp.1-18.

Reynolds-Clausen, K. and Singh, N., 2019. South Africa's power producer's revised coal ash strategy and implementation progress. Coal Combustion and Gasification Products, 11(1), pp.10-17.

Riley, K.W., 2007. Benchmarking of selected Australian and international fly ashes. *Coperative Research Centre for Coal in Sustainability Development, QCAT Technology Transfer Centre*. Pullenvale, Queensland, pp.60

Seredin, V.V. and Dai, S., 2012. Coal deposits as potential alternative sources for lanthanides and yttrium. *International Journal of Coal Geology*, *94*, pp.67-93.

Seredin, V.V., Dai, S., Sun, Y. and Chekryzhov, I.Y., 2013. Coal deposits as promising sources of rare metals for alternative power and energy-efficient technologies. Applied Geochemistry, 31, pp.1-11.

Silva, L.F., Macias, F., Oliveira, M.L., da Boit, M.K. and Waanders, F., 2011. Coal cleaning residues and Fe-minerals implications. *Environmental monitoring and assessment*, *172*(1), pp.367-378.

Sloss, L.L., 2007. *Trace elements and fly ash utilisation*. IEA Clean Coal Centre.

Spivak-Birndorf, L.J., Stewart, B.W., Capo, R.C., Chapman, E.C., Schroeder, K.T. and Brubaker, T.M., 2012. Strontium Isotope Study of Coal Utilization By-

Products Interacting with Environmental Waters. *Journal of environmental quality*, *41*(1), pp.144-154.

Taggart, R.K., Hower, J.C., Dwyer, G.S. and Hsu-Kim, H., 2016. Trends in the rare earth element content of US-based coal combustion fly ashes. *Environmental science and technology,* 50(11), pp.5919-5926.

Tang, M., Zhou, C., Pan, J., Zhang, N., Liu, C., Cao, S., Hu, T. and Ji, W., 2019. Study on extraction of rare earth elements from coal fly ash through alkali fusion–Acid leaching. *Minerals Engineering*, *136*, pp.36-42.

Taylor, S.R. and McLennan, S.M., 1985. The continental crust: its composition and evolution.

Vadapalli, V.K., Klink, M.J., Etchebers, O., Petrik, L.F., Gitari, W., White, R.A., Key, D. and Iwuoha, E., 2008. Neutralization of acid mine drainage using fly ash, and strength development of the resulting solid residues. *South African Journal of Science*, *104*(7), pp.317-322.

Van der Merwe, E.M., Prinsloo, L.C., Mathebula, C.L., Swart, H.C., Coetsee, E. and Doucet, F.J., 2014. Surface and bulk characterization of an ultrafine South African coal fly ash with reference to polymer applications. *Applied Surface Science*, *317*, pp.73-83.

Vassilev, S.V. and Vassileva, C.G., 2007. A new approach for the classification of coal fly ashes based on their origin, composition, properties, and behaviour. *Fuel*, *86*(10-11), pp.1490-1512.

Wagner, N.J. and Matiane, A., 2018. Rare earth elements in select Main Karoo Basin (South Africa) coal and coal ash samples. *International Journal of Coal Geology*, *196*, pp.82-92.

Wagner, N.J., Mokwena, M.L. and Kolker, A., 2021. Occurrence and probable source of chromium enrichment in Permian coals, South Africa. *South African Journal of Geology 2021*, *124*(3), pp.611-626.

Wang, Z., Coyte, R.M., Dwyer, G.S., Ruhl, L.S., Hsu-Kim, H., Hower, J.C. and Vengosh, A., 2020. Distinction of strontium isotope ratios between water-soluble and bulk coal fly ash from the United States. *International Journal of Coal Geology*, *222*, p.103464.

White, S.C. and Case, E.D., 1990. Characterization of fly ash from coal-fired power plants. *Journal of Materials Science*, *25*(12), pp.5215-5219.

Yang, K., Tang, Z. and Feng, J., 2020. Effect of co-use of fly ash and granular polyacrylamide on infiltration, runoff, and sediment yield from sandy soil under simulated rainfall. *Agronomy*, *10*(3), p.344.

Yao, Z.T., Ji, X.S., Sarker, P.K., Tang, J.H., Ge, L.Q., Xia, M.S. and Xi, Y.Q., 2015. A comprehensive review on the applications of coal fly ash. *Earth-Science Reviews*, *141*, pp.105-121.

Yeheyis, M.B., Shang, J.Q. and Yanful, E.K., 2008. Characterization and environmental evaluation of Atikokan coal fly ash for environmental applications. *Journal of environmental engineering and science*, *7*(5), pp.481-498.